Protein Science (1999), *8*:2312–2329. Cambridge University Press. Printed in the USA.

The role of position a in determining the stability and oligomerization state of α-helical coiled coils: 20 amino acid stability coefficients in the hydrophobic core of proteins

KURT WAGSCHAL,[1] BRIAN TRIPET,[1] PIERRE LAVIGNE,[2] COLIN MANT,[1] AND ROBERT S. HODGES[1]

[1]Department of Biochemistry and the Medical Research Council Group in Protein Structure and Function, University of Alberta, Edmonton, Alberta T6G 2H7, Canada
[2]Protein Engineering Network of Centres of Excellence, University of Alberta, Edmonton, Alberta T6G 2H7, Canada

(RECEIVED June 21, 1999; ACCEPTED August 5, 1999)

Abstract

We describe here a systematic investigation into the role of position **a** in the hydrophobic core of a model coiled-coil protein in determining coiled-coil stability and oligomerization state. We employed a model coiled coil that allowed the formation of an extended three-stranded trimeric oligomerization state for some of the analogs; however, due to the presence of a Cys-Gly-Gly linker, unfolding occurred from the same two-stranded monomeric oligomerization state for all of the analogs. Denaturation from a two-stranded state allowed us to measure the relative contribution of 20 different amino acid side chains to coiled-coil stability from chemical denaturation profiles. In addition, the relative hydrophobicity of the substituted amino acid side chains was assessed by reversed-phase high-performance liquid chromatography and found to correlate very highly ($R = 0.95$) with coiled-coil stability. We also determined the effect of position **a** in specifying the oligomerization state using ultracentrifugation as well as high-performance size-exclusion chromatography. We found that nine of the analogs populated one oligomerization state exclusively at peptide concentrations of 50 μM under benign buffer conditions. The Leu-, Tyr-, Gln-, and His-substituted analogs were found to be exclusively three-stranded trimers, while the Asn-, Lys-, Orn-, Arg-, and Trp-substituted analogs formed exclusively two-stranded monomers. Modeling results for the Leu-substituted analog showed that a three-stranded oligomerization state is preferred due to increased side-chain burial, while a two-stranded oligomerization state was observed for the Trp analog due to unfavorable cavity formation in the three-stranded state.

Keywords: α-helical coiled coil; hydrophobic core; oligomerization state; protein design; protein stability

The α-helical coiled coil, a left-handed superhelix of two or more right-handed α-helices first proposed by Crick (1953), consists of a regularly repeating heptad unit designated *abcdefg*, in which positions **a** and **d** are occupied predominately by hydrophobic amino acids and positions **e** and **g** by charged residues. The repeating pattern of hydrophobic residues in the **a** and **d** positions creates an amphipathic face where the helices pack together at an angle of ~20° with interactions **a** to **a**′ and **d** to **d**′. Residues in the **e** and **g** positions on adjacent helices are often involved in interhelical salt bridges with interactions *i* to $i' + 5$ or **g** to **e**′.

In nature, the coiled-coil motif is employed to perform a diverse array of functions, including structural roles, for example, in cytoskeletal proteins and DNA transcription factors, and dynamic roles such as pH sensitive hinges that control the release of viral particles into cells (for recent reviews, see Cohen & Parry, 1990; Alber, 1992; Hodges, 1992; Adamson et al., 1993; Baxevanis & Vinson, 1993; Betz et al., 1995; Hodges, 1996; Lupas, 1996; Kammerer, 1997; Kohn et al., 1997; Kohn & Hodges, 1998). Further, coiled coils have been predicted to occur in well over 200 proteins and will certainly be found in as-yet undiscovered protein structures. Recent inspection of the Brookhaven Protein Data Bank (PDB) has revealed that over 50 unique high-resolution structures of coiled-coil domains have been solved. It is clear, then, that identifying the occurrence of the coiled-coil motif and the structural features that modulate its overall stability, oligomerization

Reprint requests to: Robert S. Hodges, Department of Biochemistry, University of Alberta, Edmonton, Alberta T6G 2H7, Canada; e-mail: robert.hodges@ualberta.ca.

Abbreviations: CD, circular dichroism; GdnHCl, guanidine hydrochloride; HPSEC, high-performance size-exclusion chromatography; RP-HPLC, reversed-phase high-performance liquid chromatography; TFE, trifluoroethanol.

state, and specificity of heterodimerization is vital to our understanding of a diverse array of phenomena in both normal and diseased cells, as well as being important for de novo protein design applications and our general understanding of protein folding and stability (Kohn & Hodges, 1998).

In either native sequence analysis or de novo protein design, the ability to predict the stability as well as the oligomerization state, orientation of polypeptide chains (parallel or antiparallel), and preference for homodimerization or heterodimerization of coiled coils from naturally occurring or designed protein sequences is paramount. To this end, it has been established that while the factors important for stabilizing coiled coils include the α-helical propensity of the residues and the presence or absence of intrachain and interchain salt bridges, it is the nature of the hydrophobic core **a** and **d** positions that provides the greatest contribution to overall stability, as well as being important in determining oligomerization state (Hodges et al., 1990; Zhou et al., 1992a, 1992b; Harbury et al., 1993; Thompson et al., 1993; Greenfield & Hitchcock-DeGregori, 1995). However, no systematic study has yet been carried out to determine the contribution toward stability and oligomerization state that each of the 20 naturally occurring side chains can make when in the hydrophobic core. Algorithms designed to predict formation and oligomerization state of coiled-coil sequences based on the frequency of residue occurrence in a coiled-coil sequence database have been developed (Lupas et al., 1991; Berger et al., 1995; Woolfson & Alber, 1995; Lupas, 1997; Wolf et al., 1997). However, frequency of occurrence of a given amino acid side chain in a hydrophobic core position of coiled coils does not necessarily correlate with the thermodynamic stability imparted by the side chain, because a given residue can be preferred owing to the structural uniqueness engendered by the substitution, often at the expense of overall thermodynamic stability (Harbury et al., 1993; Junius et al., 1995; Lumb & Kim, 1995). This clearly renders untenable a relative stability scale for amino acid side chain substitution in the hydrophobic core based on the frequency of residue occurrence.

Hodges and coworkers designed the first model coiled-coil protein and demonstrated its utility in studying de novo design principles related to protein folding and stability (Hodges et al., 1981), and this has been followed by extensive work on the use of coiled coils to investigate principles of protein design and for biotechnology applications, recently reviewed (Hodges, 1996; Lupas, 1996; Chao et al., 1998; Kohn & Hodges, 1998). Recently, we reported the de novo design of a model coiled-coil protein termed X19**a** (Wagschal et al., 1999), which consists of two identical 38-residue (5 heptad) amphipathic helices containing the three to four hydrophobic repeat characteristic of coiled coils connected by a flexible Cys-Gly-Gly linker (Fig. 1). Our goal was the development of a model host–guest peptide sequence able to measure the relative contribution of 20 different amino acid substitutions at position **a** in the hydrophobic core toward overall coiled-coil stability and oligomerization state. Five strategically selected analogs of this model peptide sequence (Ile, Leu, Ala, Asn, and Glu analogs) were prepared to determine all of the biophysical techniques that would be required to fully characterize the coiled coils. Preliminary results suggested that this peptide sequence (Fig. 1) could indeed accept the full range of both stabilizing hydrophobic substitutions as well as potentially destabilizing hydrophilic substitutions that would be expected upon substitution with the naturally occurring amino acids (Wagschal et al., 1999).

In the present study we have substituted 14 additional naturally occurring amino acids (cysteine was omitted and ornithine was included) to obtain a complete data set for the effect on protein stability of different amino acid side chains in the hydrophobic core of two-stranded coiled coils. In addition, sedimentation equilibrium ultracentrifugation coupled with the results from HPSEC allowed us to assess the effect on resultant oligomerization state of amino acid substitution in position **a** of the central heptad of a coiled coil. Finally, we present initial modeling results that rationalize the observation of a unique oligomerization state for some analogs in terms of side-chain packing in the hydrophobic core. This is the first study to provide the effect of 20 different amino acid side chains in the hydrophobic core of a coiled-coil protein on stability and oligomerization state. These results will be extremely important in the de novo design of proteins and in predicting coiled-coil structure and stability in native proteins.

Results and discussion

Peptide design

The de novo design and complete biophysical characterization of the model peptide sequence termed X19**a** (Fig. 1) has been described in a preliminary study (Wagschal et al., 1999). Briefly, the heptad sequences used in the design were based on the amino acid sequence $E_gV_aG_bA_cL_dK_eK_f$ used in heptads 4 and 5. In heptads 1

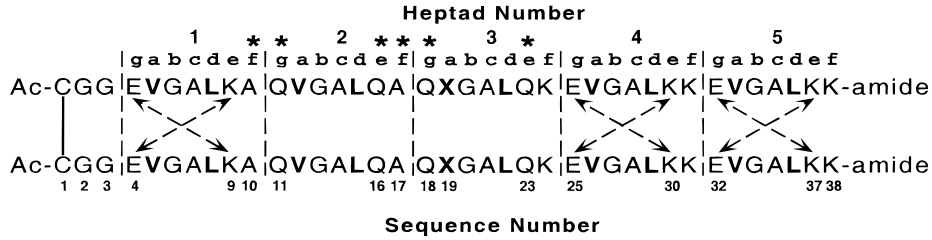

Fig. 1. Amino acid sequence of the 76-residue disulfide bridged model coiled-coil X19**a**. Each polypeptide chain consists of five heptads and the linker region (Cys-Gly-Gly). The site of amino acid substitution is denoted "X" at position 19**a**; thus, the Leu analog is denoted L19**a**, the Val analog is denoted V19**a**, etc. Vertical dashed lines separate the heptads, and dashed arrows denote interchain salt bridges in heptads 1, 4, and 5. The model heptad sequence EVGALKK was employed for heptads 4 and 5, while changes were made in the model heptad sequence in heptads 1, 2 and 3, noted by "*". To avoid intrachain and interchain i to $i + 3$ or i to $i + 4$ charge–charge interactions with the site of substitution "X," charged residues involved in **e**–**g**′ salt bridges in the standard heptad were replaced by Gln (positions 11, 16, 18, and 23). To adjust the overall charge at pH 7.0, Lys residues 10 and 17 in the standard heptad were replaced with Ala.

and 2, a Lys residue was changed to an Ala residue at position **f** to control overall charge of the peptide at neutral pH. Heptads 1, 4, and 5 provide a $Val_{\mathbf{a}}$-$Leu_{\mathbf{d}}$ hydrophobic core as well as optimal **e**–**g**′ salt bridges that help ensure parallel, in-register α-helix alignment (Monera et al., 1994). The site of substitution is at position 19**a** in the central heptad, denoted with an "**X**" in Figure 1. Gln residues replaced the Glu and Lys residues at the **e** and **g** positions in both heptads 2 and 3 to prevent interaction of charged groups with the substituted amino acid side chain. Also, Cys-Gly-Gly was added to the NH_2 terminus (O'Shea et al., 1989) to permit disulfide bond formation and to provide a flexible linker that allowed unconstrained helical alignment. This flexible linker proved to be critical because it allowed an oxidized, three-stranded trimeric state (Fig. 2b) to be observed in benign medium for some analogs. On the other hand, even though we observed a trimeric state for some of the analogs, during chemical denaturation the Cys-Gly-Gly linker allowed conversion of oxidized trimers to two-stranded oxidized monomers (Fig. 2a) prior to denaturation to the unfolded state and any loss of helicity as judged by CD (Wagschal et al., 1999). As a result, the stability data for the entire analog set described herein can be compared, because each X19**a** analog is unfolding from the same disulfide-bridged two-stranded monomeric state, to similar unfolded monomeric states.

CD spectroscopy

The CD spectrum of each oxidized analog was measured under physiologically relevant, benign buffer conditions (100 mM KCl, 50 mM PO_4, pH 7.0), and also in 50% TFE for all analogs (Table 1). The estimated maximal theoretical molar ellipticity at 222 nm and 25 °C is $-34{,}730$ deg·cm^2·dmol^{-1} for the 76-residue oxidized analogs (Chen et al., 1974; Chang et al., 1978). The analogs generally approached this maximal value under benign conditions except for Ser19**a**, Arg19**a**, Gly19**a**, Orn19**a**, Asp 19**a**, and Pro19**a**, which were 94, 78, 79, 84, 18, and 5% helical, respectively. These lower values indicate that the peptide populations of these analogs were either not completely in the folded state ($f_f < 1$), or in the case of the latter two peptides were essentially in the unfolded state under benign conditions at room temperature. To investigate whether those analogs that were not completely folded at 25 °C could, in fact, achieve a fully folded state, some of the analogs were also examined at 5 °C (Table 1). The molar ellipticity generally did not appreciably change for those analogs tested, which were completely in the folded state at 25 °C (Asn, Ala, Gln, His, Glu, and Lys). Among those analogs that were not completely in the folded state ($f_f < 1$) at 25 °C, the molar ellipticity increased by ~10% for the Ser and Arg analogs, while Gly19**a** and Orn19**a** showed a marked increase in molar ellipticity, indicating that these analogs were completely in the folded state at the lower temperature. It was especially interesting to note that Asp19**a**, which was essentially unfolded at 25 °C ($-6{,}200$ deg·cm^2·dmol^{-1}), became highly helical at 5 °C ($-32{,}300$ deg·cm^2·dmol^{-1}). Thus, at 5 °C all analogs except Pro19**a** were highly α-helical, which indicates that decreasing the temperature increases the free energy of unfolding (ΔG_u) for at least some of the analogs, thereby allowing coiled-coil formation even when the most destabilizing amino acid side chains are incorporated.

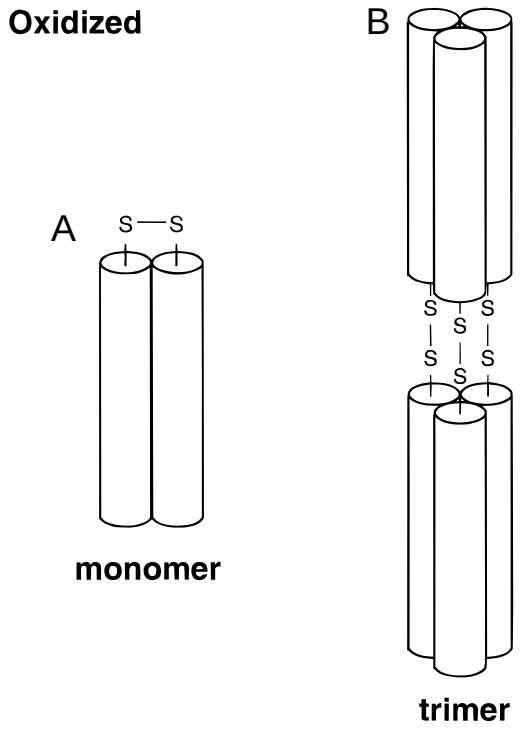

Fig. 2. Proposed models of the interchain disulfide-bridged peptides. Axial ratios obtained from sedimentation velocity experiments (Wagschal et al., 1999) indicated (**A)** the disulfide-bridged monomer is a two-stranded coiled coil, and (**B**) the disulfide-bridged trimer is an extended three-stranded coiled coil. The cylinders represent the 35-residue polypeptide chain folded as an α-helix.

Under benign conditions the ratio of ellipticities (222/208 nm) was greater than 1.0 for all of the peptides that exhibited molar ellipticities comparable to the theoretical maximum of $-34{,}700$ deg·cm^2·dmol^{-1} (Chen et al., 1974; Chang et al., 1978) (Table 1), which is indicative of the presence of interacting α-helices (Lau et al., 1984; Cooper & Woody, 1990). This ratio of ellipticities for Arg19**a**, Gly19**a**, and Orn19**a** ranged between 0.96 to 1.00, which is consistent with the observation that for these peptides $f_f < 1$ under benign conditions. However, when 222/208 nm was measured at 5 °C, the ratio was 1.03 or greater for Arg19**a**, Gly19**a**, Orn19**a**, and Asp19**a**, indicating interacting α-helices at the lower temperature, which corroborates the observation that these peptides have the ability to populate the folded state completely. It was observed that the molar ellipticity in 50% TFE at 222 nm generally decreased by about 10 to 20%. This decrease in helicity in TFE may reflect the loss of synergism in the n-π^* transition (222 nm CD band) from interacting α-helices in the coiled-coil structure (Lau et al., 1984) because TFE has been shown to disrupt tertiary and quaternary structure and to promote secondary structure (Lau et al., 1984; Cooper & Woody, 1990; Sönnichsen et al., 1992). Interestingly, the ellipticity observed in 50% TFE at 25 °C decreased significantly for Glu19**a** from $-35{,}000$ deg·cm^2·dmol^{-1} in benign buffer to $-25{,}300$ deg·cm^2·dmol^{-1} (Table 1), which suggests that charged residues are especially disruptive of α-helical structure in the form of monomeric α-helices in the nonpolar environment of TFE, compared to disruption of α-helices involved in coiled-coil structures in benign medium that are stabilized by interhelical hydrophobic interactions. The ratio of ellipticities (222/208 nm) decreased to 0.8 to 0.9 for all of the analogs (except Pro19**a**), which is characteristic of noninteracting α-helices. Pro had a devastating effect on coiled-coil structure ($-1{,}900$ deg·cm^2·dmol^{-1}) compared to the monomeric α-helix in 50%

Table 1. *CD spectroscopy data*

Substituted amino acid[a]	$[\Theta]_{222}$[b] 25 °C benign	% α-Helix[c] 25 °C benign	$[\Theta]_{222}$[b] 5 °C benign	$[\Theta]_{222}$[d] 25 °C 50% TFE	$[\Theta]_{222/208}$[e] 25 °C benign	$[\Theta]_{222/208}$[e] 5 °C benign	$[\Theta]_{222/208}$[e] 25 °C 50% TFE
Ile*	−36,100	104	—	−30,800	1.06	—	0.90
Val	−38,200	110	—	−33,100	1.03	—	0.90
Met	−34,800	100	—	−33,600	1.06	—	0.89
Leu*	−36,600	105	—	−33,300	1.03	—	0.89
Phe	−34,300	99	—	−30,200	1.04	—	0.88
Tyr	−36,700	106	—	−33,200	1.05	—	0.89
Trp	−39,900	115	—	−32,400	1.04	—	0.84
Asn*	−34,500	99	−33,500	−33,600	1.03	1.07	0.91
Thr	−39,300	116	—	−28,900	1.06	—	0.85
Ala*	−34,800	100	−36,400	−30,200	1.08	1.11	0.85
Gln	−35,300	102	−33,500	−29,300	1.04	1.08	0.85
His	−37,200	107	−36,700	−32,800	1.04	1.08	0.85
Lys	−37,600	108	−36,800	−28,400	1.02	1.06	0.83
Ser	−32,800	94	−36,700	−29,300	1.03	1.07	0.84
Arg	−27,100	78	−30,300	−22,600	1.00	1.03	0.82
Gly	−27600	79	−35,800	−28,300	1.00	1.09	0.82
Orn	−29,100	84	−36,300	−31,000	0.96	1.05	0.83
Glu*	−35,900	103	−38,000	−25,300	1.07	1.10	0.83
Asp	**−6,200**	18	**−32,300**	−24,500	0.56	1.05	0.80
Pro	**−1,900**	5	**−1,900**	−20,300	0.24	0.24	0.77

[a] Substituted amino acid at position 19**a** denotes the corresponding disulfide bridged coiled coil. See Figure 1 for peptide amino acid sequence. The asterisk (*) indicates previously reported in Wagschal et al. (1999).

[b] Mean residue molar ellipticities at 222 nm ($deg \cdot cm^2 \cdot dmol^{-1}$). Measurements were performed on ~50 μM samples of disulfide-bridged peptide in benign buffer (100 mM KCl, 50 mM PO_4, pH 7.0) at the indicated temperature.

[c] The % α-helix at 25 °C was calculated based on an ellipticity value of −34,730 $deg \cdot cm^2 \cdot dmol^{-1}$ for a 100% helical 35-residue peptide derived from the equation $X_H^n = X_H^\infty(1 - k/n)$ where H_n^∞ is −39,500 $deg \cdot cm^2 \cdot dmol^{-1}$ for a helix of infinite length, n is the residue number per helix, and k is a wavelength dependent constant (2.5 at 222 nm) (Chen et al., 1974; Chang et al., 1978).

[d] Mean residue molar ellipticities at 222 nm ($deg \cdot cm^2 \cdot dmol^{-1}$) in 50% TFE. Measurements were performed at ~50 μM on oxidized peptide in benign buffer diluted 1:1 (v/v) with TFE.

[e] A ratio of $[\Theta]_{222/208}$ greater than 1.0 is a measure of interacting α-helices in benign media, and a ratio of ~0.90 represents noninteracting α-helices in 50% TFE (Lau et al., 1984).

TFE (−20,300 $deg \cdot cm^2 \cdot dmol^{-1}$). This is in excellent agreement with previous studies on monomeric α-helices where essentially 0% α-helix was observed in benign buffer and 50% α-helix was observed in 50% TFE (Zhou et al., 1994).

Side-chain hydrophobicity

Intuitively it is thought that the more hydrophobic the amino acid side chain substituted in the hydrophobic core, the more stable the resultant coiled coil. This suggestion has been supported by mutational studies in globular proteins (Matthews, 1993; Richards & Lim, 1994) and coiled coils (Hodges et al., 1990; Zhu et al., 1993; Moitra et al., 1997). In the present study we investigated this relationship, and reversed-phase HPLC (RP-HPLC) was used to measure the hydrophobicity of the substituted amino acid side chains because interaction of the amphipathic faces of the α-helices to form the coiled coil in benign buffer is analogous to the interaction of the amphipathic face (preferred binding domain) of the α-helices with the reversed-phase C8 stationary phase (Zhou et al., 1990). Moreover, while the relative hydrophobicity of the amino acid side chains has been determined previously in other model systems (Fauchère & Pliska, 1983; Guo et al., 1986; Monera et al., 1995), it was necessary to assess whether the relative hydrophobicity remained the same in the context of the amino acid sequence employed in the present study. The peptides were *S*-carboxamidomethylated to preclude re-oxidation of the cysteine residues during analysis, and RP-HPLC was performed at 70 °C to prevent aggregation (which causes peak broadening and multiple peaks) of the Ile analog on the HPLC column observed at room temperature. The separation was also performed at 25 °C, the temperature at which the chemical denaturation experiments were performed, and the same elution order was observed except for Ile19**a**. The RP-HPLC method used to determine side-chain hydrophobicity resulted in all of the analogs being well resolved under the elution conditions employed (Fig. 3; Table 2), with a 17.4 min difference in retention times between the most hydrophilic analog (Asp19**a**, t_R = 47.2 min) and the most hydrophobic analog (Leu19**a**, t_R = 64.6 min). RP-HPLC separation of the analogs was performed individually as well as in three sets, with the common peptide A19**a** in each set as a retention time reference (Fig. 3).

A summary of the side-chain hydrophobicity results is shown in Table 2. Comparison of these retention times with the relative order of hydrophobicity previously observed in a monomeric α-helix model system where the hydrophobic face consists of Ala residues except at the substitution site (Monera et al., 1995) reveals an excellent correlation (R = 0.98) of relative hydrophobicity (Fig. 4A). This indicates that the hydrophobicity of the amino acid side chains substituted at position 19**a** is model independent under RP-HPLC

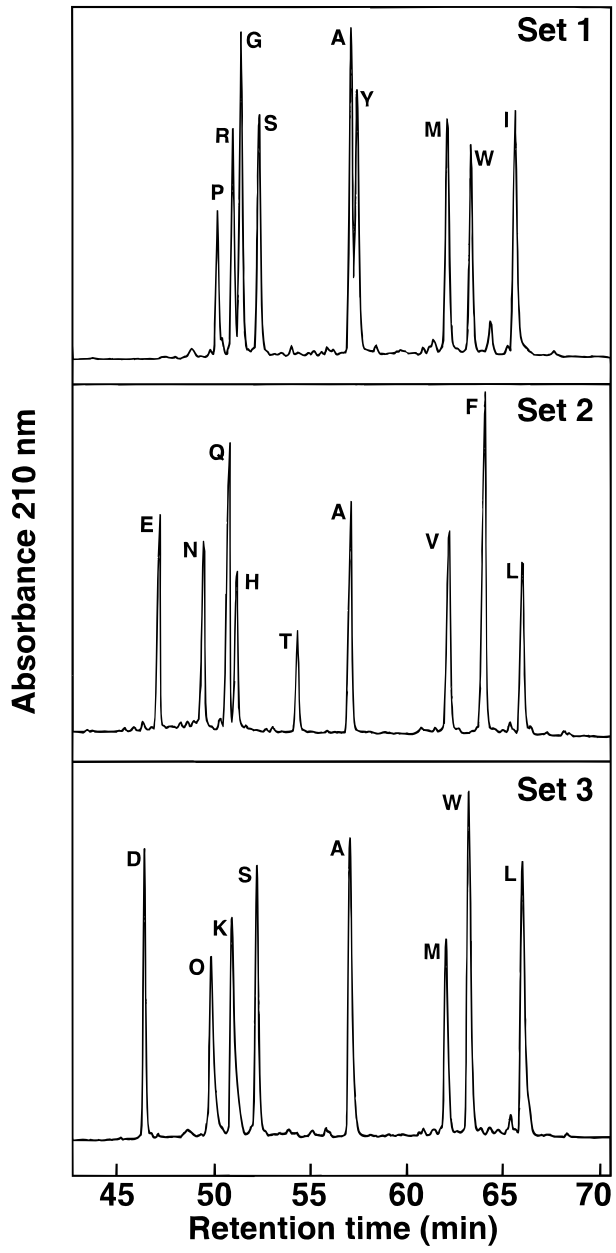

Fig. 3. RP-HPLC separation of each analog to determine relative side-chain hydrophobicity at pH 7.0. The corresponding N-terminal *S*-carboxamidomethyl cysteine derivatives of the peptides were prepared to prevent oxidation, and chromatography was performed at 70 °C to prevent aggregation. Separation was carried out using a Zorbax 300 XDB C8 reversed-phase column as described in Materials and methods. Peptide A19**a** was included in each analog set as an internal reference standard, and the resulting retention times are shown in Table 2.

conditions. Comparison of the retention times with those obtained from random coil peptides (Fig. 4B) (Guo et al., 1986) likewise revealed a very high correlation ($R = 0.95$), indicating the hydrophobicity of a substituted side chain measured when in an α-helix (Fig. 4A) is not perturbed by the structural context in which it occurs. Finally, the relative hydrophobicity values also correlated well ($R = 0.91$) with ΔG(transfer) values calculated by Eisenberg and McLachlan (1986) from hydrophobic parameters of amino acids side chains measured by Fauchère and Pliska (1983), where ΔG(transfer) is the free energy of transfer of the acetylated amino acid amide between an aqueous medium and octanol (Fig. 4C). Thus, these results, taken together, reveal that the differences in hydrophobicity between analogs is due solely to the change in the hydrophobicity of the substituted amino acid side chain. An exception is the analog Pro19**a**, which had a much lower retention time (Fig. 4B,C) than would be indicated by either the ΔG(transfer) value or from its hydrophobicity measured in random-coil peptides where the Pro- and Ala-substituted analogs had identical hydrophobicities. This can be understood, because it is known that the carboxamidomethylated analogs partition as monomeric α-helices during RP-HPLC (Blondelle et al., 1995). The extremely helix-disrupting nature of the proline residue, in fact, introduces random-coil character, thereby disrupting the preferred binding domain, and resulting in a decrease in RP-HPLC relative retention time for this analog.

Protein stability

A major goal of this study was to develop a relative stability scale, and because it was not possible to denature thermally all of the analogs (vide infra), it was necessary to employ chemical denaturation to determine relative stability. Thus, each peptide was denatured at pH 7.0 using both GdnHCl and urea denaturant in separate experiments, and the change in molar ellipticity at 222 nm was monitored using CD spectroscopy. Both GdnHCl and urea were used in the present study because the specific contribution to protein stability of the ionic interactions can be unmasked in urea (Monera et al., 1993; Kohn et al., 1995). Moreover, it has also been shown that using more than one method of denaturation can reveal the presence of potentially stable (populated) folding intermediates (Morjana et al., 1993). It is important to note that it has previously been shown that the oxidized analogs that form three-stranded species under benign conditions (either exclusively or in conjunction with two-stranded species) undergo a transition to an exclusively two-stranded monomeric state prior to a loss of helicity as measured by CD spectroscopy (Wagschal et al., 1999). This characteristic of model peptide sequence X19**a** is crucial because it allows comparison of the effect on stability of side-chain substitution on a two-stranded oxidized monomer for all the analogs regardless of the oligomerization state observed in benign medium.

The urea and GdnHCl denaturation curves obtained are shown in Figure 5. The relative order of stability was generally the same in both denaturants, with the hydrophobic amino acid substituted analogs being the most stable, the charged residue substituted analogs the least stable, and the polar side-chain substituted analogs being of intermediate stability (Table 3). The transitions were monophasic using either GdnHCl or urea, with single inflection points observed for all analogs, consistent with a monomolecular two-state unfolding process in both denaturants with intermediate states minimally populated. The transition midpoints were between 0.3 and 3.3 M in GdnHCl, and between 0.6 and 7.6 M in urea (Table 3). Comparison of the midpoints obtained in the two denaturants revealed an excellent correlation ($R = 0.99$) between denaturant midpoints (Fig. 6A), with the more chaotropic reagent, GdnHCl, being about twice as effective a denaturant as urea.

The change in free energy of unfolding for each of the analogs relative to the Ala substituted peptide, $\Delta\Delta G_u$(Ala), was measured using the GdnHCl and urea denaturation data as described in Materials and methods (Table 3). The importance of the hydrophobic core in modulating overall protein stability was reflected in the

Table 2. *Side-chain hydrophobicity data determined from amphipathic α-helical peptides, random-coil peptides and N^{α}-acetyl amino acids*

	Leu/Val face analogs (this study)			Ala face analogs	Random-coil analogs	
Substituted amino acid[a]	t_R[b] (min)	Δt_R(Gly)[c] (min)	Δt_R(Gly)[d] (normalized)	Δt_R(Gly)[e] (normalized)	Δt_R(Gly)[f] (normalized)	ΔG(trans)[g] (kcal/mol)
Leu*	64.6	13.1	100	100	100	2.32
Ile*	64.3	12.8	98	101	92	2.46
Phe	62.8	11.3	86	103	100	2.44
Trp	62.2	10.7	82	100	105	3.07
Val	61.2	9.7	74	78	64	1.66
Met	61.1	9.6	73	76	67	1.68
Tyr	56.9	5.4	41	64	52	1.31
Ala*	56.7	5.2	40	42	26	0.42
Thr	54.2	2.7	21	13	5	0.35
Ser	52.3	0.8	6	−5	−3	−0.05
Gly	51.5	0	0	0	0	0.00
His	51.4	−0.1	−1	8	26	0.18
Arg	51.2	−0.3	−2	−14	12	−1.37
Lys	51.2	−0.3	−2	−24	0	−1.35
Gln	51.0	−0.5	−4	−11	2	−0.30
Pro	50.5	−1.0	−8	−29	26	0.98
Orn	50.2	−1.3	−10	—	—	—
Asn*	49.9	−1.6	−12	−29	−7	−0.82
Glu*	47.8	−3.7	−28	−32	−12	−0.87
Asp	47.2	−4.3	−33	−57	−26	−1.05

[a] Substituted amino acid at position 19**a** denotes the corresponding disulfide bridged coiled coil. See Figure 1 for peptide amino acid sequence. The asterisk (*) indicates previously reported in Wagschal et al. (1999).

[b] t_R is the RP-HPLC retention time (pH 7.0 running buffer) of the X19**a** analogs (Fig. 3), where the cysteine residue in each peptide was derivatized to *S*-carboxamidomethyl cysteine. See Materials and methods for derivatization and separation conditions.

[c] Δt_R(Gly) is the difference in the RP-HPLC retention time of analog X19**a** relative to the Gly-substituted analog. The nonpolar face of this coiled-coil sequence consists of Val and Leu residues except at the substitution site.

[d] The normalized Δt_R(Gly) values from this study, where the Δt_R value for Leu19**a** = 100 and for Gly19**a** = 0.

[e] The normalized Δt_R(Gly) values of a substituted 18-residue monomeric amphipathic α-helix where the nonpolar face consists of Ala residues except at the substitution site from Monera et al. (1995), where the Δt_R value for the Leu-substituted analog = 100 and that for the Gly-substituted analog = 0.

[f] The normalized Δt_R(Gly) values of a substituted eight-residue random-coil peptide from Guo et al. (1986), where the Δt_R value for the Leu-substituted analog = 100 and that for the Gly-substituted analog = 0.

[g] ΔG(trans) is the free energy of transfer between octanol and water for the amino acid side chain relative to glycine (from Eisenberg & McLachlan, 1986).

observation that a single amino acid mutation in peptide sequence X19**a** modulated the stability over a substantial 6 to 7 kcal/mol range (Table 3). The correlation of $\Delta\Delta G_u$(Ala) values obtained using the two denaturants was also excellent ($R = 0.97$) (Fig. 6B). These results indicate that the relative stabilities of the analogs to chemical denaturation is nearly the same for each denaturant. However, the $\Delta\Delta G_u$(Ala) value obtained using urea as a denaturant for the charged side-chain analog Glu19**a** was significantly lower than that obtained from the corresponding GdnHCl denaturation experiment ($\Delta\Delta G_u$(Ala) = −3.64 kcal/mol in urea and −1.98 kcal/mol in GdnHCl; Table 3, Fig. 6B). This observation is consistent with some shielding of ionic interactions of the negatively charged Glu carboxylate group at pH 7.0 due to ion pairing with the guanidinium ion (Kohn et al., 1995). As reported previously, the GdnHCl derived stabilities may provide a better value for the relative contribution of the hydrophobic interactions to coiled-coil stability, whereas urea denaturation studies allow the measurement of the net stability conferred by a given amino acid side chain to overall protein stability (hydrophobic and charged interactions) (Monera et al., 1994). Thus, while comparable results were obtained using either GdnHCl or urea, the stability values obtained using urea provided the best measure of the effect of charged amino acid side-chain substitution on overall stability.

As described previously, the model X19**a** coiled-coil scaffold was designed to accept even the most destabilizing substitutions and still fold into a coiled-coil structure (Wagschal et al., 1999). Even so, we observed that Asp19**a** was essentially denatured at room temperature and was fully folded only when the temperature was lowered to 5 °C (Table 2). Due to the high inherent stability of the coiled-coil scaffold, it was possible to obtain thermal denatur-

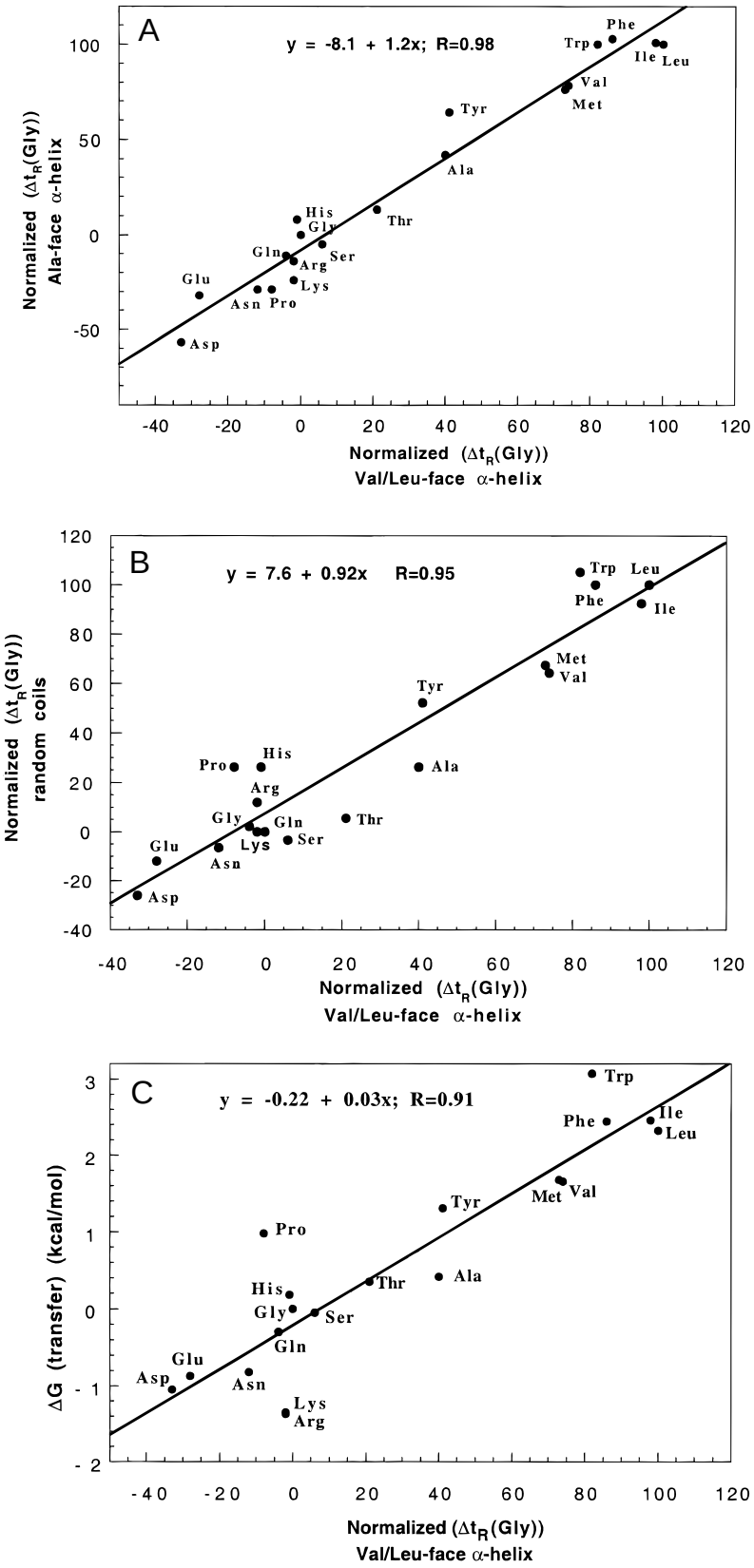

Fig. 4. Correlation of side-chain hydrophobicity data. **A:** Correlation of Δt_R(Gly) data obtained in a previous study by Monera et al. (1995) using an Ala-face α-helical peptide with Δt_R(Gly) obtained in the present study using the Val/Leu-face peptide X19**a**. **B:** Correlation of Δt_R(Gly) data obtained in a previous study by Guo et al. (1986) using a random coil peptide with Δt_R(Gly) from this study. **C:** Correlation of ΔG(transfer), the free energy of partitioning N-acetyl amino acid amides between a polar aqueous environment and octanol (from Eisenberg & McLachlan, 1986) and Δt_R(Gly) (from this study).

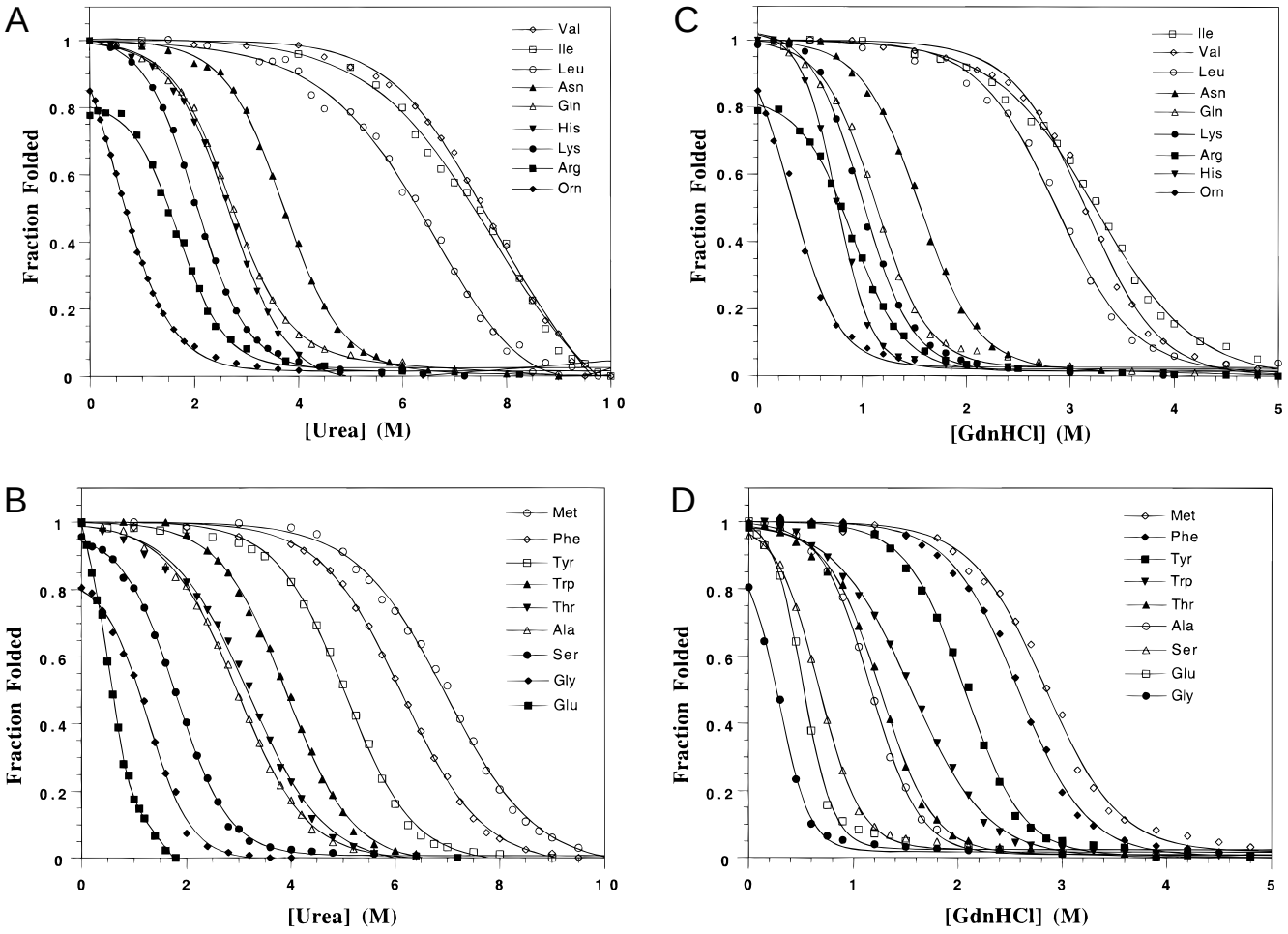

Fig. 5. Chemical denaturation profiles. **A, B:** Urea denaturation profiles. **C, D:** GdnHCl denaturation profiles. **A** and **C** show the denaturation profiles for the Val, Ile, Leu, Asn, Gln, His, Lys, Arg, and Orn analogs, and **B** and **D** show the denaturation profiles for the Met, Phe, Tyr, Trp, Thr, Ala, Ser, Gly, and Glu analogs. A fraction-folded value of 1.0 corresponds to a negative molar ellipticity of 34,300 or greater in benign medium at 25 °C.

ation profiles for only the less stable analogs. Figure 7 shows the relationship between the thermal and chemical denaturation midpoints for those analogs that folded at room temperature and for which it was possible to obtain thermal denaturation profiles in benign buffer. The T_m values obtained for the less stable analogs in benign buffer are shown in Table 3, and they varied from 8.4 °C for Asp19**a** to 65.3 °C for Thr19**a**. It has previously been shown (Su et al., 1994) that the T_m values for a series of especially stable coiled coils measured in the presence of increasing concentrations of denaturant resulted in a linear relationship between the concentration of denaturant and T_m for each peptide, thus allowing calculation of an extrapolated T_m in the absence of denaturant in each case. Thus, while it was not possible to denature the Ile analog thermally in the absence of denaturant, in this study the T_m of Ile19**a** was measured in the presence of 3, 4, and 5 M urea (data not shown), and an extrapolated T_m value of 108 °C in benign buffer was obtained (Fig. 7). Using both this extrapolated T_m for Ile19**a** and the T_m values for the less stable analogs measured in benign buffer, an excellent correlation was obtained ($R = 0.99$) between T_m and $[\text{urea}]_{1/2}$, though Asn 19**a** is a clear outlier and was not used in calculating the correlation coefficient. Extrapolated T_m values for the more stable analogs (Table 3) were calculated using the best-fit linear relationship from Figure 7 ($T_m = 11.325[\text{urea}]_{1/2} + 26.336$), and these ranged from 71 °C for Trp19**a** to 112 °C for Val19**a**.

Comparison of side-chain hydrophobicity and protein stability

The effect on overall stability of mutating residues in the hydrophobic core of a coiled coil or other protein is dependent on the difference in hydrophobicity of the amino acid side chains, termed the hydrophobic effect, and the difference in the van der Waals interactions upon mutation, termed the packing effect (Eriksson et al., 1992). When the urea stability data ($\Delta\Delta G_u$ (Urea, Ala)) and the side-chain hydrophobicity data [Δt_r(Ala)] were compared, it was found that, in general, the stability of the X19**a** analogs directly correlated with hydrophobicity of the substituted side chain ($R = 0.94$, Fig. 8a), with Asn19**a** and Trp19**a** being clear outliers (vide infra). Thus, four of the six most hydrophobic side chains in the present study are also the four most stable X19**a** analogs, which in order of descending stability are V, I, M, and L (Table 3). In a

Table 3. *Stability and oligomerization state data*

Substituted amino acid[a]	Urea			GdnHCl			Oligomerization data[e]		
	$[Urea]_{1/2}$[b] (M)	Slope[c] (m)	$\Delta\Delta G_u$(Ala)[d] (kcal/mol)	$[GdnHCl]_{1/2}$[b] (M)	Slope[c] (m)	$\Delta\Delta G_u$(Ala)[d] (kcal/mol	Trimer (%)	Monomer (%)	T_m[f] (°C)
Ile*	7.40	0.58	3.29	3.26	1.18	3.88	39	61	[110]
Val	7.56	0.62	3.51	3.17	1.58	4.10	57	43	[122]
Met	6.94	0.77	3.31	2.85	1.53	3.43	90	10	[105]
Leu*[g]	6.39	0.60	2.97	2.90	1.49	3.48	**100**	0	[99]
Phe	6.15	0.83	2.76	2.57	1.74	3.01	65	35	[96]
Tyr	5.02	0.93	1.89	2.07	2.09	2.08	**100**	0	[87]
Trp	3.91	1.01	0.90	1.54	1.65	0.78	0	**100**	[71]
Asn*	3.73	0.96	0.71	1.54	1.94	0.85	0	**100**	53.6
Thr	3.18	0.86	0.18	1.25	2.13	0.20	76	24	65.3
Ala*	2.97	0.91	0	1.17	2.53	0	38	**62**	62.3
Gln	2.74	0.94	−0.21	1.11	2.20	−0.13	**100**	0	59.1
His	2.64	1.11	−0.33	0.77	3.24	−1.15	**100**	0	58.0
Lys	2.05	1.13	−0.93	0.98	1.84	−0.40	0	**100**	44.7
Ser	1.80	1.11	−1.17	0.67	2.66	−1.28	25	75	49.3
Arg	1.51	1.00	−1.39	0.81	1.81	−0.77	0	**100**	41.7
Gly	1.08	1.01	−1.81	0.27	3.03	−2.49	35	65	38.3
Orn	0.68	1.31	−2.53	0.34	2.00	−1.88	0	**100**	30.9
Glu*	0.60	2.17	−3.64	0.52	3.61	−1.98	46	54	33.9
Asp	—	—	—	—	—	—	—	—	8.4
Pro	—	—	—	—	—	—	—	—	—

[a] Substituted amino acid at position 19**a** denotes the corresponding disulfide bridged coiled coil. See Figure 1 for peptide amino acid sequence. The asterisk (*) indicates previously reported in Wagschal et al. (1999).

[b] $[denaturant]_{1/2}$ is the denaturation profile transition midpoint.

[c] m is the slope in the equation $\Delta G_u = \Delta G_{H_2O} + m[denaturant]$ (Pace, 1986) with units $kcal \cdot mol^{-1} \cdot M^{-1}$.

[d] $\Delta\Delta G_u$(Ala) is the free energy of unfolding of the analog relative to the Ala-substituted analog and is calculated from the equation $\Delta\Delta G_u(Ala) = \{(m_{Ala} + m_2)/2\}\{([denaturant]_{1/2})_{peptide} - ([denaturant]_{1/2})_{Ala}\}$ (Sali et al., 1991). Denaturation occurred from the same two-stranded monomeric state for each analog (Wagschal et al., 1999), and the $\Delta\Delta G_u$(Ala) values reported are for two substitutions (one in each α-helix). Positive values indicate stabilities greater than that of the Ala-substituted analog.

[e] Percentages of monomer and trimer observed by analyzing an aliquot of a 50 μM peptide in benign buffer by HPSEC as described in Materials and methods. Those analogs that populate exclusively either monomeric or trimeric association states in benign media are bold.

[f] T_m is the midpoint of the thermal denaturation profiles in benign buffer (50 mM KH_2HPO_4, 100 mM KCl pH 7.0) for the oxidized analogs. Values in brackets [ ] are extrapolated values obtained from measured $[urea]_{1/2}$ values using the best-fit linear equation from the data in Figure 7; T_m [extrapolated] = $11.325[urea]_{1/2} + 26.336$.

[g] Denaturation of L19**a** was performed at peptide concentrations of 5.6 μM for the urea denaturation experiment and 2.5 μM for the GdnHCl denaturation experiment to ensure unfolding from a monomeric oligomerization state. Denaturation of all other analogs was performed at peptide concentrations of 50 μM.

two-stranded coiled coil, the position **a** side chains display packing geometries with the Cα–Cβ bond pointing out of the hydrophobic core, while the position **d** amino acid Cα–Cβ bond points directly at the adjacent α-helix (Harbury et al., 1993). As a result, β-branched amino acid side chains can be more stable in an **a** position than residues of similar or even greater hydrophobicity that are not β-branched and also more stable than the same β-branched amino acid in a **d** position. We in fact observed that Ile19**a** was more stable than Leu19**a** due to this favorable packing effect, even though Leu is more hydrophobic (Table 2). These results are in agreement with previous studies, in which it was shown that mutating Leu to Ile at position **a** in coiled coils showed a significant packing effect in stabilizing coiled coils, with $\Delta\Delta G_{Ala}$ values ranging from 0.59 to 1.03 kcal/mol (Zhu et al., 1993). These results lend credence to the host/guest strategy employed because the model system was able to probe these differences in β-branched amino acid side-chain packing. Vinson and coworkers have recently reported a study designed to measure the energetic contribution to stability of six different amino acids in the hydrophobic core **d** position of a dimeric leucine zipper coiled coil, and they found that the order of descending stability as determined by thermal denaturation experiments was L, M, I, V, C, A (Moitra et al., 1997). Thus, their results demonstrated that Leu is the most stabilizing amino acid in the **d** position, in agreement with previous studies by Hodges and coworkers (Zhu et al., 1993), which is consistent with side-chain packing at a **d** position favoring Leu rather than β-branched amino acids in two-stranded coiled coils.

It is generally accepted that the hydrophobic effect is the main factor in stabilizing the folded structure of globular proteins. Experiments designed to address this hypothesis have been performed in which Leu has been changed to Ala, with resultant decreases in stability that ranged from 1.7 to 6.2 kcal/mol (Matthews, 1993). The lower value is comparable to the difference in the solvent transfer free energy [$\Delta\Delta G$(transfer)] of 1.9 kcal/mol between the methyl and *t*-butyl side chains of Ala and Leu (Table 2), which is solely due to differences in hydrophobicity of

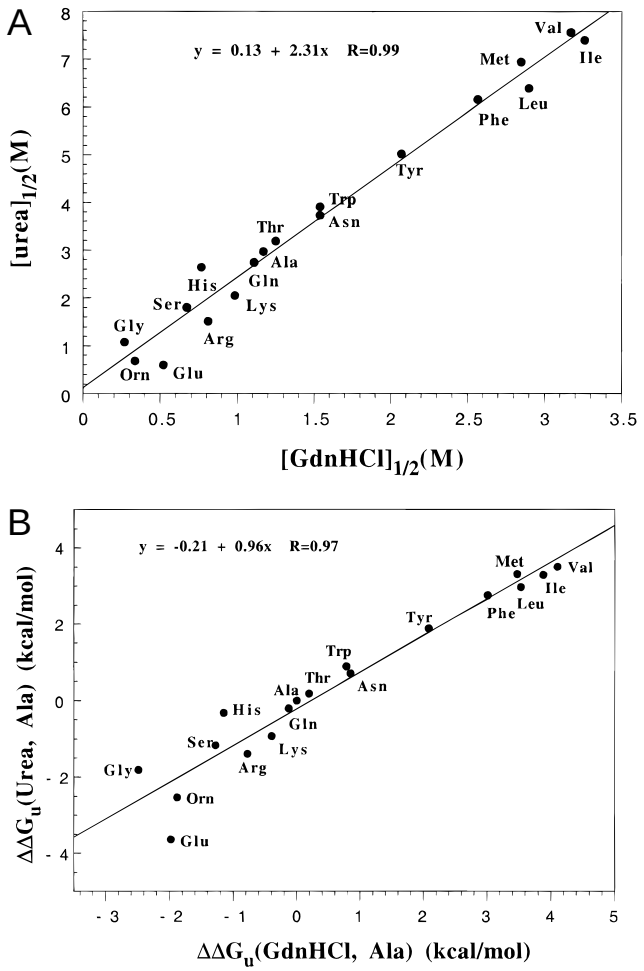

Fig. 6. Comparison of chemical denaturation midpoints and relative stabilities obtained using GdnHCl and urea. **A:** Correlation of urea and GdnHCl chemical denaturation profile midpoints. **B:** Correlation of $\Delta\Delta G_u$(Ala) measured in GdnHCl and urea. The free energy of unfolding relative to the Ala-substituted analog was measured using the equation: $\Delta\Delta G_u(\text{Ala}) = \{(m_{\text{Ala}} + m_2)/2\}\{([\text{denaturant}]_{1/2})_2 - ([\text{denaturant}]_{1/2})_{\text{Ala}}\}$ (Sali et al., 1991).

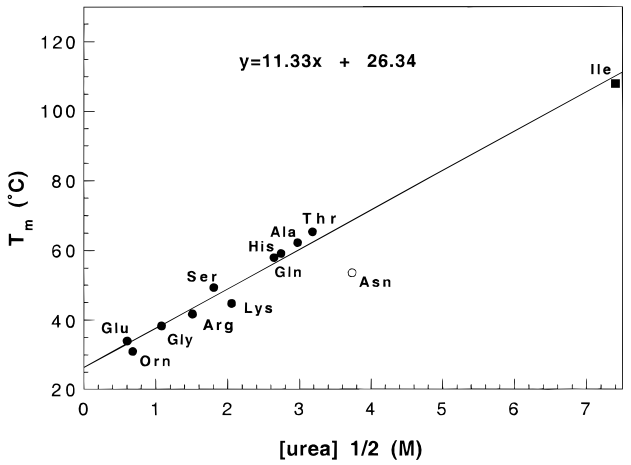

Fig. 7. Comparison of thermal and chemical denaturation midpoints, T_m and $[\text{urea}]_{1/2}$. The T_m value in benign buffer for the Ile analog (closed square, 108°C) was obtained by extrapolating the T_m values measured in 3, 4, and 5 M urea to zero denaturant concentration (Su et al., 1994). The T_m values for the other analogs used in calculating the best linear fit (closed circles) were obtained in benign media. The Asn analog (open circle) was a clear outlier and was not used in calculating the correlation coefficient, $R = 0.99$.

the Leu and Ala side chains (Fauchère & Pliska, 1983). The wide range between this lower value and the upper value has been ascribed to differences in the size of the cavity created when the Leu side chain is replaced with a methyl group, with the loss in stability correlating with the increase in cavity volume caused by the mutation (Eriksson et al., 1992). In the present study, the value of 1.6 kcal/mol/mutation observed for Leu → Ala substitution is comparable to the $\Delta\Delta G$(transfer). This loss of stability is also comparable to that observed previously by Zhou et al. (1992), where mutation of two leucine residues at the corresponding position of a similar model coiled-coil protein resulted in a 1.8 kcal/mol/mutation loss in stability. This suggests that the differences in stability between the Leu and Ala analogs is mainly due to differences in side-chain hydrophobicity, and that the two position **a** Ala side chains can pack in a two-stranded coiled coil without forming a cavity.

The Trp19**a** analog was observed to be ~2.3 kcal/mol less stable than would be predicted by relative hydrophobicity (Fig. 8A), indicated by the "+" sign in Figure 8B. Modeling suggests that this is due to nonoptimized burial of the hydrophobic moiety of the side chain. As seen in Figure 11B, the benzyl moiety of the side chain is exposed to the solvent, while Nϵ1 of the indole ring is buried in the two-stranded coiled-coil (Fig. 11B). Thus, while contributing greatly to the hydrophobicity of the side chain as measured by RP-HPLC, the six-membered ring of the indole moiety is not appreciably desolvated in the coiled-coil structure. In contrast, Tyr, Gln, and His substitutions result in coiled coils that are more stable (denoted by "+" signs in Fig. 8B) than would be expected based on side-chain hydrophobicity/hydrophilicity alone. Modeling of these residues in a two-stranded coiled-coil structure (modeling not shown) reveals that only the hydrophobic regions of these side chains are buried, while the polar hydroxyl moiety of Tyr, the imidazole nitrogens of His, and the Gln carboxamide group can remain at least partly solvated. However, the hydrophobicity measured by RP-HPLC for these side chains entails desolvation of both the nonpolar and polar regions of the Tyr, Gln and His side chains in the reversed-phase matrix. Thus, side-chain burial in the isotropic reversed-phase matrix and in the coiled-coil hydrophobic core are not equivalent for the polar side chains where selective desolvation of the more nonpolar region of the side chain can occur in the protein fold. The Asn-substituted coiled coil was also significantly more stable than indicated by its low relative hydrophobicity (denoted by a "+" sign in Fig. 8B). This can be understood, because the carboxamide moiety of Asn can H-bond at the hydrophobic interface of the coiled coil (O'Shea et al., 1991; Harbury et al., 1993; Lumb & Kim, 1995; Lavigne et al., 1997, 1998; Greenfield et al., 1998), unlike in the C8 RP-HPLC matrix where these H-bonds do not form.

Lysine at the **a** position of coiled coils has been seen to occur in leucine zippers (Glover & Harrison, 1995; Gonzalez et al., 1996c). Modeling shows that the side chain bearing the positively charged ϵ-amino group of Lys19**a** in a two-stranded coiled coil is long enough to extend out of the hydrophobic core and allow at least partial solvation. The ornithine analog (Orn19**a**), the homologue of

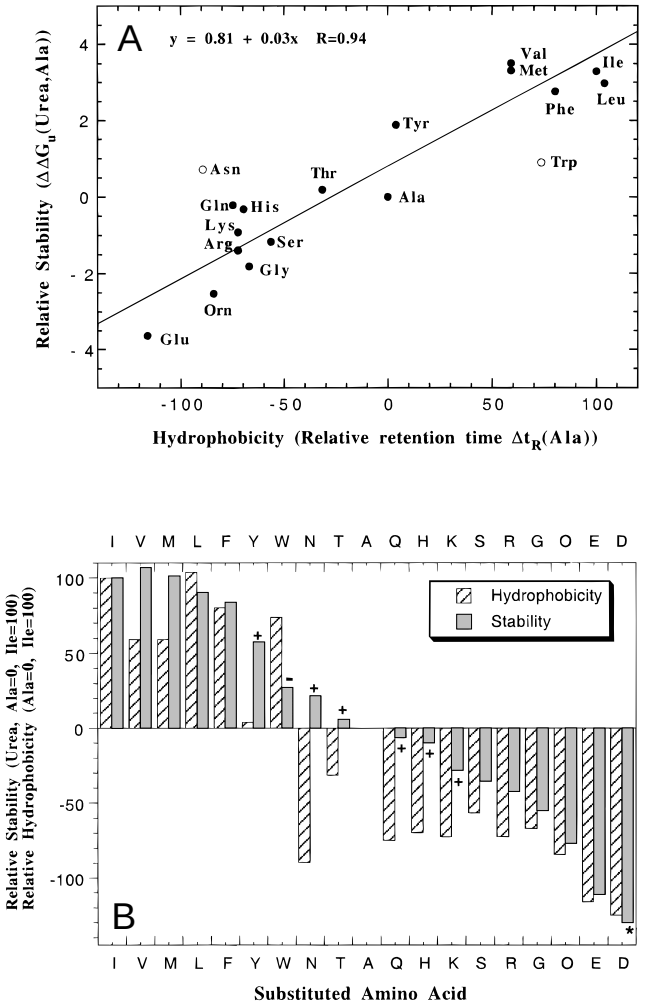

Fig. 8. Correlation of side-chain hydrophobicity and relative stability. **A:** Correlation of relative free energy of unfolding obtained from the urea denaturation experiments, $\Delta\Delta G_u$(Urea, Ala), with the RP-HPLC retention time of the analogs relative to the Ala-substituted analog, Δt_R(Ala). The analogs used for linear extrapolation and calculation of the correlation coefficient are shown as closed circles, while the analogs substituted with Asn and Trp were outliers and were not used in the calculations, and are shown as open circles. **B:** Histogram representation of relative stability obtained from urea denaturation experiments, normalized such that the stability of Ile = 100 and Ala = 0, and the relative hydrophobicity obtained from RP-HPLC retention time data, normalized such that the hydrophobicity of Ile = 100 and Ala = 0. Analogs having a stability greater than twofold of that indicated by apparent side-chain hydrophobicity are denoted "+" (Y, N, Q, T, H, and K), while the analog (W) having a stability less than twofold of that indicated by apparent side-chain hydrophobicity is denoted "−". *The coiled coil with Asp at position 19**a** was fully folded in benign medium at 5 °C but unfolded at room temperature (Table 1) with T_m of 8.4 °C (Table 3). The star denotes that the Asp19**a** coiled coil is considerably less stable than Glu19**a**, and its $urea_{1/2}$ value could not be determined at 25 °C.

Lys19**a** in which the substituted side chain bearing the positively charged amino group is shortened by one methylene group, served to probe the effect of bringing the charged amino group closer to the peptide backbone. As seen in Figure 8A and in Table 3, Orn19**a** was 1.5 kcal less stable than Lys19**a** as measured in urea denaturation experiments. While Orn19**a** is slightly less hydrophobic than Lys19**a**, there is an additional decrease in stability observed above that expected due solely to decreased hydrophobicity. This observation is consistent with the δ-amino group of Orn being less solvated due to its closer proximity to the hydrophobic core.

Although Glu was the most destabilizing amino acid substitution that still allowed coiled-coil formation under benign condition at room temperature, and Asp19**a** achieved a fully folded state only when the temperature was lowered to 5 °C (Table 1), the acidic residues Glu and Asp do indeed occur in coiled coils (Lupas et al., 1991). Destabilizing residues such as Asp and Glu can play an important role in controlling the preferential formation of heterodimeric species over homodimeric species in vivo because the presence of acidic side chains at the dimerization interface is an effective mechanism to destabilize the incipient homodimer. For example, the basic region helix-loop-helix leucine zipper (b-HLH-LZ) oncoprotein c-Myc must preferentially heterodimerize with the b-HLH-LZ Max protein to bind DNA and activate transcription. Homodimerization of the c-Myc protein is prevented (and heterodimerization thus promoted by mass action) by two Glu residues at **a** positions (Muhle-Goll et al., 1994; Lavigne et al., 1995), and, in fact, the leucine zipper domains of all the proteins known to date that interact with Max have a conserved acidic residue (either Glu or Asp) in the dimerization interface. In addition to disfavoring homodimer formation, these conserved acidic residue side chains are also part of a molecular recognition mechanism that actively promotes specific heterodimer formation. Thus, recent NMR solution structure work by Lavigne and coworkers on the DNA binding c-Myc-Max heterodimer (Lavigne et al., 1998) showed conclusively that the previously postulated electrostatic interactions (Lavigne et al., 1995) between the two position **a** Glu side chains in the c-Myc leucine zipper and a position **d** His side chain in the Max leucine zipper are indeed responsible for the specificity of heterodimer formation. Glu is also seen in the hydrophobic core of kinesin molecules where it occurs in close proximity to Lys or Arg residues. The local environment is, therefore, more favorable than if substituted into the context of a strictly aliphatic hydrophobic core, and this context dependent modulation of stability has been suggested to be important in conferring upon the motor protein the ability to carry out selectively a movement signal (Tripet et al., 1997).

Examination of the *m* values (Table 3), which are a measure of denaturant effectiveness for a given protein, revealed that the analogs fell into three groups; those containing very hydrophobic substitutions had the lowest *m* values, those with the most hydrophilic substitutions had the highest *m* values, and the remainder of the analogs displayed intermediate *m* values. The *m* values in GdnHCl were in general about twice those measured in urea. In a study in which denaturant *m* values from a large set of proteins was examined, it was found that *m* correlated ($R = 0.87$ for GdnHCl) with the change in solvent accessible surface area (ASA) upon unfolding (Myers et al., 1995). The variation in *m* values can therefore be ascribed to differences in the unfolded states of the analogs, which is relevant because the denatured states of the analogs are equal in importance to the native states in determining protein stability (Muñoz & Serrano, 1996). Thus, higher *m* values observed with the hydrophilic residues could be associated with unfolded states possessing relatively greater ASA and less residual structure, while the lower *m* values observed with the hydrophobic side-chain–substituted analogs are associated with unfolded states having relatively less ASA and more residual structure. In summary, it appears that hydrophobic amino acid substitution may lead to increased residual structure in the unfolded state.

Protein stability vs. natural occurrence of amino acids at position **a**

Comparing the frequency of occurrence of amino acid residues at position **a** in naturally occurring coiled coils (Lupas et al., 1991) with their relative stability in model X19**a** from this study shows that the amino acid side chains of the four most stable analogs (I19**a**, V19**a**, M19**a**, and L19**a**) also occur frequently at position **a** (Fig. 9). Thus, the stability of naturally occurring coiled coils is predominately provided by highly hydrophobic side chains in the hydrophobic core. Also, Gly and Glu, which give rise to the two least stable analogs, occur relatively infrequently at position **a**. In contrast to the highly hydrophobic amino acid side chains, Figure 9 shows that there is no clear relationship between stability and frequency of occurrence for the side chains of intermediate hydrophobicity. For example, Phe, Trp, Thr, Gln, and His substitutions resulted in coiled coils of appreciable stability, yet these residues are not used to a great extent in naturally occurring coiled coils. This may be partly due to some amino acids being not as prevalent in nature owing to the metabolic cost associated with their biosynthesis, and the use of some amino acids to control the oligomerization state rather than stability. Thus, we found that with the exception of Phe and Trp, nature has preferentially chosen hydrophobic amino acids for position **a**, thus providing maximal stability. The lack of a clear correlation between stability and frequency of occurrence for some of the analogs underscores the importance of the stability data obtained using our model peptide sequence in the present study for de novo design applications and for the creation of algorithms designed to predict the occurrence and stability of coiled coils in naturally occurring peptides and proteins.

Oligomerization state

The structural polymorphism (oligomerization) of coiled-coil–forming peptides has been documented previously (Gonzalez et al., 1996a, 1996b, 1996c; Hodges, 1996). More relevant to this study are the examples of single amino acid replacement of the hydrophobic core position **a** wild-type Asn residue in the exclusively two-stranded GCN4 coiled coil (Gonzalez et al., 1996a, 1996b, 1996c; Hodges, 1996). To date the Ala, Abu (aminobutyric acid), Gln, Nrl (norleucine) and Lys mutants have been characterized structurally (X-ray crystal structure) and hydrodynamically (oligomerization state). Only the wild-type Asn and the Lys mutant are known to populate exclusively the two-stranded state in that system (Gonzalez et al., 1996c), while all the other mutants are known to populate both the two- and three-stranded states (Gonzalez et al., 1996a, 1996b; Hodges, 1996).

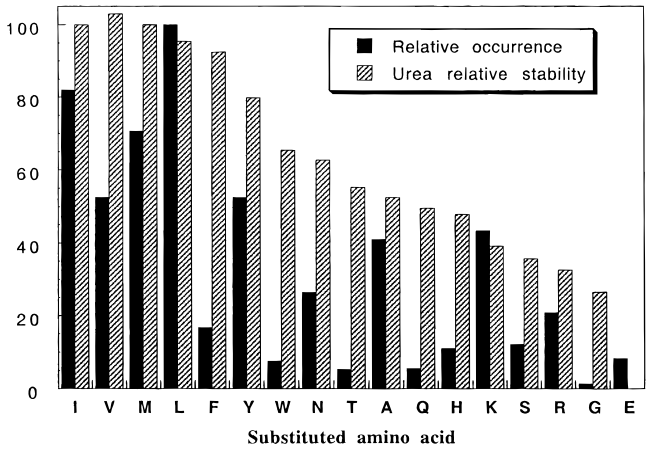

Fig. 9. Comparison of side-chain occurrence with relative side-chain stability. The relative stability obtained from urea denaturation experiments (Table 1) are normalized, with the stability of the Ile analog equal to 100, and that of the Glu analog equal to 0. The relative occurrence of the substituted amino acids in the hydrophobic core "**a**" position of coiled coils (Lupas et al., 1991) are also normalized, with the occurrence of Leu equal to 100 and that of Glu equal to 0.

The oligomeric state(s) populated by the different analogs from the present study under benign conditions are presented in Table 3. The oligomerization state of the analogs under benign conditions was determined by HPSEC, and the molecular weights of the HPSEC peaks assigned as monomers (two-stranded) or trimers (three-stranded) was confirmed by sedimentation equilibrium ultracentrifugation. Representative sedimentation equilibrium results for Lys19**a**(ox) and Tyr19**a**(ox), which populate exclusively monomeric and trimeric association states, respectively, are shown in Figure 10. These results corroborated the HPSEC data by showing that Lys19**a**(ox) was best fit as a single species monomer (calculated M_r 7,634, observed M_r 7,975; Fig. 10) and that Tyr19**a**(ox) was best fit as a single species trimer (calculated M_r 23,112, observed M_r 20,840, Fig. 10) throughout the concentration range imposed by the sedimentation equilibrium run ($\sim$50 to $\sim$500 μM). The quaternary structure of the oligomers was previously assessed in sedimentation velocity experiments that showed the oxidized peptides employed throughout this study formed two-stranded monomers (Fig. 2A) and elongated three-stranded trimers (Fig. 2B) (Wagschal et al., 1999). We found that amino acid substitution at a single hydrophobic core "**a**" position in the 5-heptad model coiled coil could switch the oligomerization state from exclusively monomeric to exclusively trimeric, with 9 of the 19 substitutions directing the oligomerization state to a unique two- or three-stranded conformation (Table 3). This clearly demonstrates the importance of the effect of packing in the hydrophobic core on oligomerization state. Thus, at protein concentrations equivalent to those under which the chemical denaturation experiments were carried out (50 μM) and under benign conditions, Leu19**a**, Tyr19**a**, Gln19**a**, and His19**a** were found to be exclusively three stranded (trimeric), while Asn19**a**, Lys19**a**, Orn19**a**, Arg19**a**, and Trp19**a** were exclusively two stranded (monomeric). These results are especially relevant for our understanding of the polymorphism of coiled coils and its prediction because they increase the database to all proteogenic amino acids except Cys at position **a** in a model peptide.

Although it is clear from these results that the hydrophobic core is very important in determining the oligomerization state of the coiled coils, it should be noted that the observed oligomerization states may be modulated, because positions **e** and **g** are also involved in the hydrophobic interface and have been shown to play a role in determining oligomerization state (Alberti et al., 1993; Beck et al., 1997; Zeng et al., 1997; Kammerer et al., 1998; Kohn et al., 1998). On the other hand, it is of particular interest to note that we also observe two-stranded specificity for the Asn and Lys analogs, which supports the general applicability of the oligomerization state results from this study. This structural specificity imparted by Asn and Lys has been ascribed to the destabilization of the three-stranded state by unoptimized buried H-bonds (Asn) and unfavorable desolvation of the charged Nϵ amino group of Lys

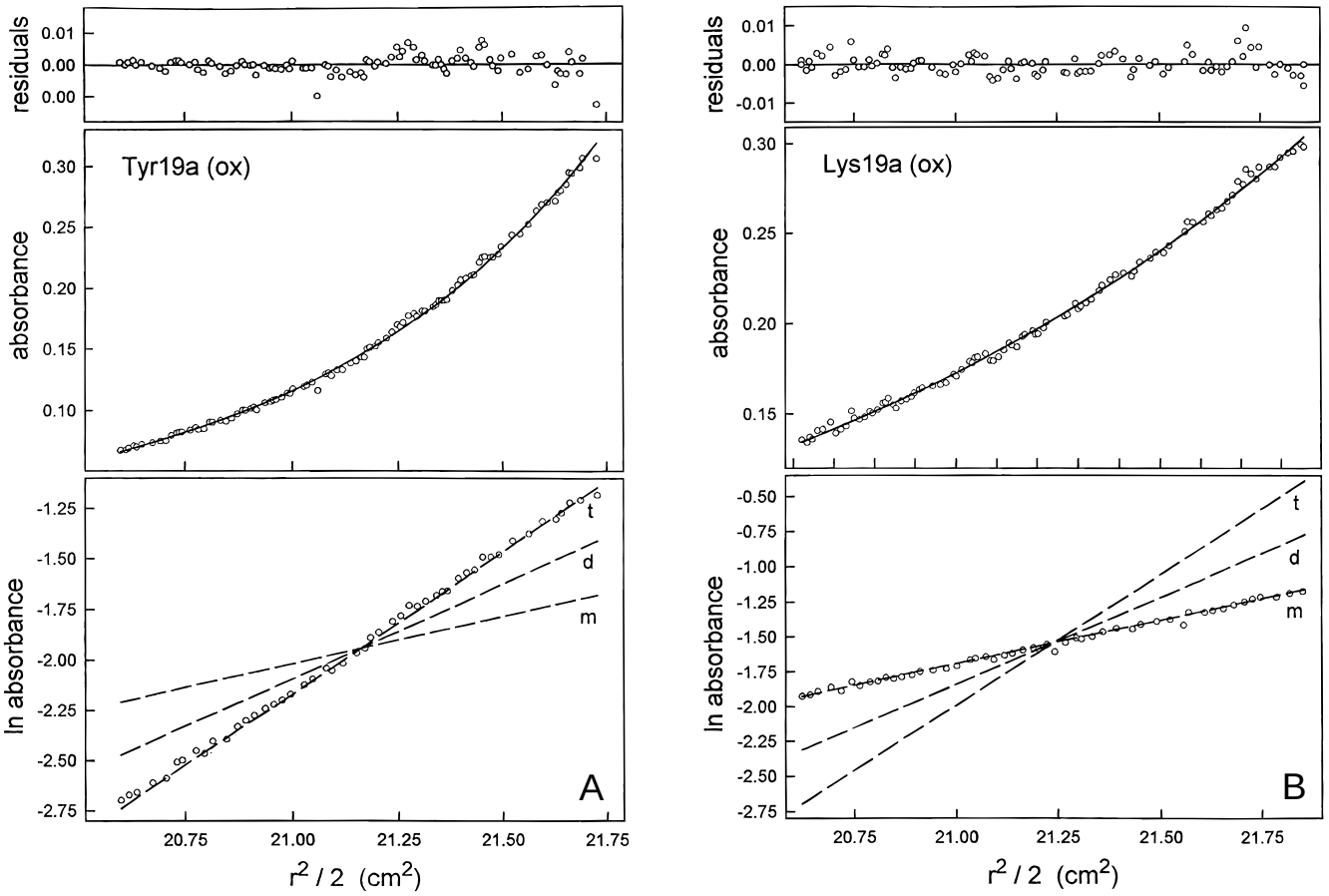

Fig. 10. Sedimentation equilibrium analysis of Lys19a(*ox*) and Tyr19a(*ox*). Sample loading concentration was 200 μM. The middle panels (absorbance vs. radius) show the best fits for a single-species monomeric curve fit for Lys19**a**(*ox*) (28K rpm) and a single-species trimeric curve fit for Tyr19**a**(*ox*) (24K rpm). The upper panels show the residuals from the curve fits, and the lower panels show ln absorbance vs. r^2 of the data (open circles) compared to theoretical monomer (m), dimer (d), and trimer (t) single-species plots (broken lines).

(Gonzalez et al., 1996c). These unfavorable events are relieved in the two-stranded state where the Asn can form an interhelical side-chain H-bond, and the Nϵ amino group of Lys is more favorably solvated (Gonzalez et al., 1996c). This selective destabilization of one state can be seen as a general mechanism for the structural specificity imparted by some of the side chains. Hence, it could be predicted [and as proposed by others (Gonzalez et al., 1996c)] that the Arg analog should show the same specificity for a two-stranded state, and, in fact, this is observed here for both the Arg and Orn analogs. Although it is tempting to suggest that all the analogs that are potentially charged at pH 7.0 should show specificity for a two-stranded structure, it is interesting to note the Glu analog is an exception in that both the two- and three-stranded states are populated. However, the pK_a of Glu side-chain carboxylate group at this position may be perturbed and must be determined before an explanation for this observation can be proposed.

Modeling of Trp and Leu in two- and three-stranded coiled coils

Our current efforts on the modeling of the Leu analog in both two- and three-stranded oligomerization states (Fig. 11A,C) indicate that the Leu side chains pack asymmetrically in the two-stranded state ($\chi1 = gauche+$, $\chi2 = trans$, and $\chi1 = trans$, $\chi2 = gauche-$) to satisfy good van der Waals interaction (avoid the formation of a cavity). In the three-stranded state, it is also possible to avoid cavity formation and optimize the packing of side chains that adopt an asymmetric arrangement (two side chains with $\chi1 = gauche+$, $\chi2 = trans$, and one with $\chi1 = trans$, $\chi2 = gauche-$). Interestingly, the Leu side chains in the two-stranded state are on average 82% buried, while they are 96% buried in the three-stranded state, suggesting in part why this analog selectively folds as a three-stranded coiled coil. The calculation of the accessible surface area of Ile side chains at position **a** in two- and three-stranded states reveals similar extents of side-chain burial as observed for the Leu analog. Nevertheless, the Ile analog is observed to populate both the two- and three-stranded states. This can be rationalized, however, because the conformational entropy penalty for Ile side-chain burial is significantly larger than that incurred for Leu side-chain burial (Lee et al., 1994). This should destabilize the three-stranded state of the Ile analog (making it relatively less populated) to the advantage of the two-stranded state.

Side-chain packing in relation to cavity formation is also an important consideration in determining the oligomerization state.

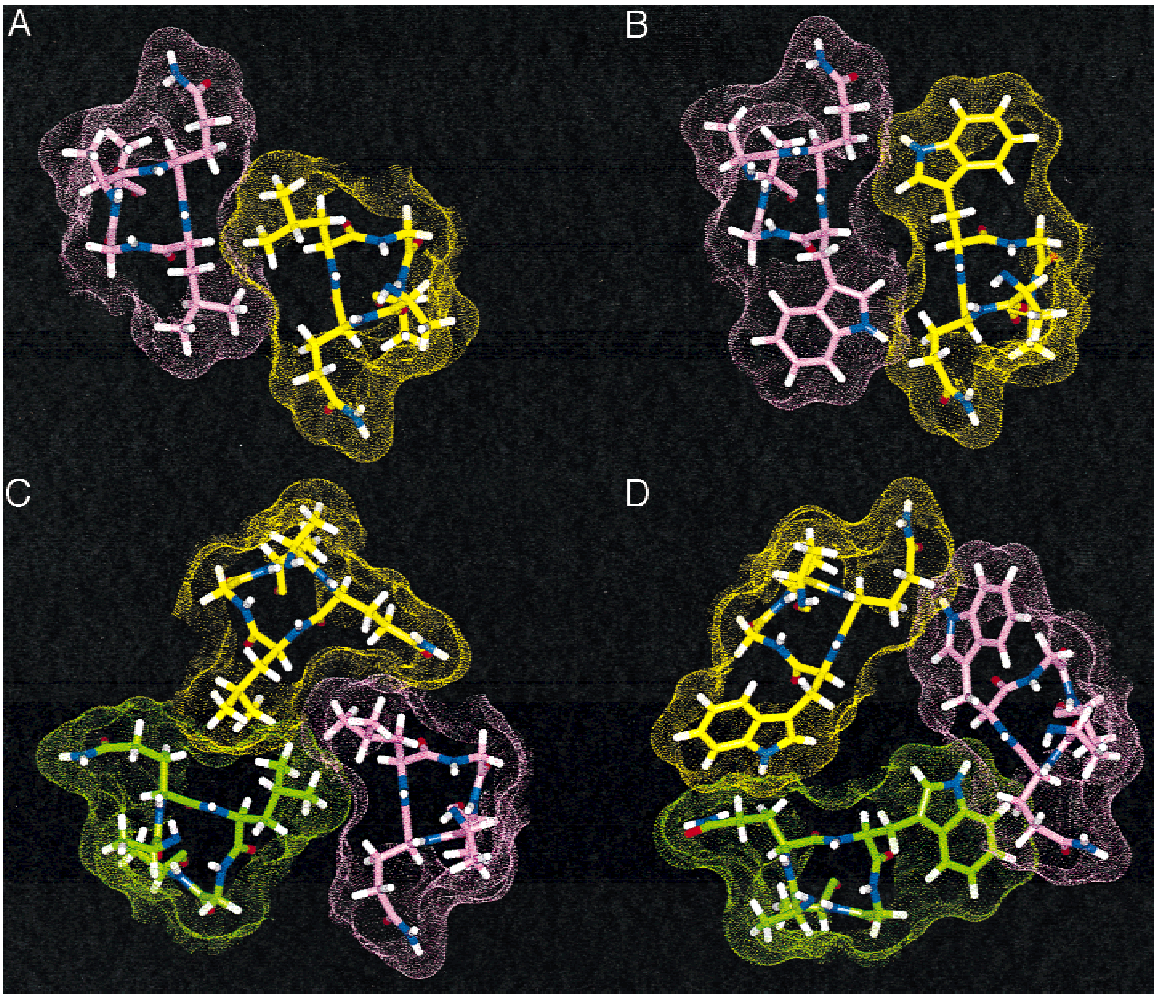

Fig. 11. Modeling of the Leu and Trp analogs as two- and three-stranded coiled coils. Good side-chain packing was obtained for both the two- and three-stranded conformations of the Leu analog (**A** and **C**, respectively). However, an exclusively three-stranded conformation is observed in benign media due to increased side-chain burial in the three-stranded state (96% burial in the three-stranded fold compared to 82% burial in the two-stranded state). Modeling of the Trp analog in two- and three-stranded conformations (**B** and **D**, respectively) shows that the three-stranded state is highly disfavored due to the formation of a large cavity (114 $Å^3$), resulting in an exclusively two-stranded oligomerization state.

Previously, Hodges et al. showed that the oligomerization state of coiled coils can be modulated by the relative positioning of Ala residues in the hydrophobic core (Monera et al., 1996). They found that the small Ala side-chain methyl group controls the formation of two- or four-stranded α-helical coiled coils by creating a large cavity if four Ala residues are on the same plane, which disfavors tetramer formation and results in a two-stranded coiled coil. Gonzalez et al. (1996b) used the principle of cavity formation leading to lowered stability to engineer an allosteric switch in GCN-4. They changed the position 16**a** Asn residue to Ala, and the resulting coiled coil was found to populate both two- and three-stranded oligomerization states. A nearly exclusively three-stranded structure was formed upon addition of benzene or cyclohexane, which was shown in high-resolution structures to fill a cavity created in the three-stranded structure by substitution of the smaller Ala side chain. Similarly, the packing effect of placing the large indole ring of Trp in the hydrophobic core is also important in controlling resultant oligomerization state. Modeling of Trp19**a** in both two- and three-stranded conformations (Fig. 11B,D) shows that packing of the bulky indole ring side chain in a three-stranded conformation is highly unfavorable due to the formation of a large cavity (114 $Å^3$), and this is likely the driving force causing the formation of exclusively two-stranded molecules for this analog. In agreement with this proposal is the observation that in the synthetic peptide coil Ser, the antiparallel orientation of one of the three helices in the bundle was due to the inability to pack three Trp residue side chains in the same core layer (Lovejoy et al., 1993). However, while Trp does not pack well and is, in fact, somewhat destabilizing relative to its hydrophobicity, Trp does, in fact, occur in the hydrophobic core of natural coiled coils (Lupas et al., 1991) and has been shown to affect, for example, inter-helix spacing in gp41 trimers (Weissenhorn et al., 1997). Thus, the presence of the large Trp side chain in the core contributes to helix orientation and protein function, as well as to oligomerization state.

Mixtures of two- and three-stranded coiled coils were observed for nine of the analogs under benign conditions (Table 3), and the

observation of multiple conformations from a single sequence implies that the two- and three-stranded structures have comparable stabilities (Dill et al., 1995). The mixture of two- and three-stranded oligomerization states observed for the Asn16Ala GCN4 mutant of Gonzalez et al. (1996) mentioned previously was also observed for the Ala analog in this study (Table 3). It has been reported that a GCN4 leucine zipper mutant in which Asn16 was changed to Abu could exist in either both two- or three-stranded coiled-coil conformations, and high-resolution structures showed that the mutant was accommodated in the two distinct structures by utilizing different residues in each conformation to form similarly shaped packing surfaces (Gonzalez et al., 1996a). It seems likely that a similar phenomenon is responsible for the polymorphism observed in the present study.

Distinctive residue propensities (frequencies of occurrence) for oligomerization states agreed with our experimentally measured effects of amino acid substitution on our model coiled-coil protein for only some of the analogs that exhibited unique oligomerization states. Thus, Asn, Lys, and Arg occur 2.4×, 6.9×, and 12.9×, respectively, more often at the "**a**" position of two-stranded coiled coils than three-stranded coiled coils, while Gln occurs 11.8 times more in three-stranded coiled coils than in two-stranded coiled coils (Woolfson & Alber, 1995). However, for the Leu19**a** analog there was a nearly equal occurrence of the residues in two- and three-stranded coiled coils (1.5τ in preference for the dimer), while Trp occurred only once in the database and was actually found in a parallel three-stranded molecule. Thus, as shown earlier in relation to overall coiled-coil stability, differences in the statistical occurrence of a given residue at position **a** of two- and three-stranded coiled coils does not necessarily predict the actual oligomerization state.

Conclusion

These findings are the first comprehensive quantitative assessment of the effect on the stability of two-stranded coiled coils of side-chain substitution in the hydrophobic core, and also provide information on the effect of side-chain hydrophobicity and packing in the hydrophobic core on oligomerization state. This study will be invaluable for the development of coiled-coil predictive algorithms and may also find use in estimating the stability of heterodimers. The effects on stability and oligomerization state of amino acid substitution observed in our model coiled coil in general corroborate results previously made using natural protein sequences, which shows that the data obtained using this host/guest system will be generally applicable. Side-chain packing as a determinant of the relative stability of alternative oligomerization states appears to be crucial, as illustrated by the molecular modeling of the Leu- and Trp-substituted analogs in the present study. Efforts to model all 20 analogs in both two- and three-stranded oligomerization states are in progress, and these results will be presented in detail elsewhere.

Materials and methods

Peptide synthesis and purification

The peptide analogs were synthesized by solid phase peptide synthesis methodology and purified by RP-HPLC, as described elsewhere (Wagschal et al., 1999). The cysteine *S*-carboxamidomethyl derivatives were prepared by treating a 1 mg/mL solution of the peptide in 50 mM NH_4HCO_3 buffer, pH 7.8, with a 10-fold excess of iodoacetamide as previously described (Chong & Hodges, 1982). The disulfide-bridged coiled coils were formed by overnight air oxidation at room temperature of ~10 mg/mL peptide in 100 mM NH_4HCO_3, pH 8.5. All peptides were characterized by analytical HPLC and electrospray mass spectrometry, and protein concentrations as well as amino acid composition were determined by amino acid analysis.

CD spectroscopy

Circular dichroism (CD) spectroscopy was performed using a Jasco J-500C spectropolarimeter (Jasco, Easton, Maryland). A 10-fold dilution of an ~500 μM stock solution of the disulfide-linked peptide was loaded into a 0.02 cm fused silica cell and ellipticity scanned from 190 to 250 nm. Each disulfide-bridged analog was analyzed by CD spectroscopy under benign conditions (50 mM phosphate, 100 mM KCl, pH 7.0) and also in the presence of 50% TFE in the same buffer. Also, some analogs were also similarly scanned at 5 °C under benign conditions. For temperature denaturation studies, the stock peptide solutions were diluted with appropriate volumes of buffer and denaturant (urea) when required. Wavelength and time scans were recorded after 10 min of equilibration of the sample at different temperatures. The molar ellipticity at 222 nm was used to monitor unfolding over the temperature range from 4 to 85 °C.

HPLC

Side-chain hydrophobicity was determined using RP-HPLC at pH 7.0. The corresponding N-terminal cysteine *S*-carboxamidomethyl derivatives of the peptides were analyzed at 70 °C. Derivatization of the free cysteine thiol group in conjunction with HPLC analysis at elevated temperature served to prevent both oxidation and aggregation. The elution buffers contained 100 mM $NaHClO_4$ to minimize nonspecific interaction with deprotonated silanol species on the column. Chromatography was carried out using a Zorbax 300 XDB-C8 column (4.6 × 150 mm) and a linear AB gradient of 1% B/min, where buffer A was aqueous 100 mM $NaClO_4$, 50 mM KH_2PO_4, pH 7.0, and buffer B was a 1:1 mixture of acetonitrile and aqueous 200 mM $NaClO_4$, 100 mM KH_2PO_4, pH 7.0.

Chemical denaturation studies

The stability of each model X19**a** analog was determined at 25 °C using CD spectroscopy by monitoring ellipticity at 222 nm during chemical denaturation using either GdnHCl or urea. A 10 M stock solution of urea and a 8 M stock solution of GdnHCl were prepared in 50 mM phosphate, 100 mM KCl buffer, pH 7.0, and aliquots were used to prepare a series of peptide solutions that were ~50 μM in different concentrations of denaturant. The peptide was incubated overnight in the GdnHCl denaturation experiments, and for at least 30 min in the urea denaturation experiments. The ellipticities of the peptides at the different denaturation concentrations were recorded at 222 nm. The fraction of peptide in the folded state (f_f) was calculated from the equation $f_f = ([\theta]_{obs} - [\theta]_u)/([\theta]_n - [\theta]_u)$, where $[\theta]_{obs}$ is the observed mean residue ellipticity at any given denaturant concentration and $[\theta]_n$ and $[\theta]_u$ are the mean residue ellipticities for the native (folded) and un-

folded states, respectively. The ΔG_u for the unfolding of a monomeric two-stranded coiled coil,

$$F = U,$$

was calculated using

$$\Delta G_u = -RT \ln(f_u/(1 - f_u))$$

where $f_u = (1 - f_f)$.

The measurement of $\Delta G_u^{H_2O}$ (the free energy of unfolding in the absence of guanidine hydrochloride) and slope m were performed by extrapolating from the free energy of unfolding (ΔG_u) at each denaturant concentration to zero concentration assuming a linear model (Pace, 1986):

$$\Delta G_u = \Delta G^{H_2O} - m[\text{GdnHCl}].$$

The main purpose of the study was to determine the relative difference in free energy of unfolding between analogs ($\Delta\Delta G_u$). $\Delta\Delta G_u$ was calculated relative to alanine [$\Delta\Delta G_u$(Ala)] because the Ala-substituted analog has the smallest side chain, with the exception of the glycine analog, and moreover, had intermediate $\Delta G_u^{H_2O}$ and slope (m) terms ideal for use as the reference values. We calculated $\Delta\Delta G_u$(Ala) using the equation:

$$\Delta\Delta G_u(\text{Ala}) = \{(m_{\text{Ala}} + m_2)/2\} \times \{([\text{denaturant}]_{1/2})_{\text{peptide}} - ([\text{denaturant}]_{1/2})_{\text{Ala}}\}$$

(Sali et al., 1991), where m_{Ala} and m_2 are the slope terms and $[\text{denaturant}]_{1/2}$ is the denaturant concentration at the transition midpoint.

Sedimentation equilibrium studies

Sedimentation equilibrium runs (48 h) were performed at 20 °C using a Beckman XL-I analytical ultracentrifuge with rotor speeds of 20K, 24K, and 28K rpm, and peptide loading concentrations of 200, 100, and 50 μM. Samples were first dialyzed exhaustively against benign buffer at 4 °C. The partial specific volumes of the peptides were calculated to be 0.7623 mL/g for Lys19**a**(*ox*) and 0.7581 mL/g for Tyr19**a**(*ox*) using the method of Cohn and Edsall and the program Sednterp (Cohn & Edsall, 1943; Wishart et al., 1994), and the density of the solvent was calculated to be 1.009 g/mL. Absorbance optics with detection at 242 nm and six-sector charcoal-filled Epon sample cells were used, and measurements were performed following the procedures outlined in the XLI Instruction Manual (Beckman Instruments, Inc., 1997). The sedimentation equilibrium data were evaluated using a nonlinear least-squares curve-fitting algorithm (Johnson et al., 1981) contained in the NonLin analysis program (Yphantis, 1991).

Structural modeling

The models for the Leu and Trp analogs in the dimeric and trimeric states were generated by replacing the proper residues in the GCN4 Asn16Gln dimeric (1ZIL) and trimeric (1ZIM) crystal structures using the program InsightII (InsightII 97, MSI). The side chains were repacked manually while monitoring for clashes using the Biopolymer module of the InsightII suite. The final sets of rotamers (*trans*, *gauche*+, and *gauche*−) for the replacement and surrounding side chains were selected on the basis of the absence of interatomic clashes and cavities as verified using the program GRASP (Nicholls et al., 1991).

Acknowledgments

We thank Kimio Oikawa and Leslie Hicks for excellent technical assistance and helpful discussions in CD spectroscopy and analytical ultracentrifugation. We gratefully acknowledge the Medical Research Council of Canada for supporting this research.

References

Adamson JG, Zhou NE, Hodges RS. 1993. Structure, function and application of the coiled-coil protein folding motif. *Curr Opin Biotechnol 4*:428–437.

Alber T. 1992. Structure of the leucine zipper. *Curr Opin Genet Dev 2*:205–210.

Alberti S, Oehler S, von Wilcken-Bergmann B, Müller-Hill B. 1993. Genetic analysis of the leucine heptad repeats of Lac repressor: Evidence for a 4-helical bundle. *EMBO J 12*:3227–3236.

Baxevanis AD, Vinson CR. 1993. Interactions of coiled coils in transcription factors: Where is the specificity? *Curr Opin Genet Dev 3*:278–285.

Beck K, Gambee JE, Kamawal A, Bächinger HP. 1997. A single amino acid can switch the oligomerization state of the α-helical coiled-coil domain of the cartilage matrix protein. *EMBO J 16*:3767–3777.

Beckman Instruments, Inc. 1997. *Optima XL-I analytical ultracentrifugation instruction manual*. Palo Alto, CA: Spinco Business Center of Beckman Instruments, Inc.

Berger B, Wilson DB, Wolf E, Tonchev T, Milla M, Kim PS. 1995. Predicting coiled coils by use of pairwise residue correlations. *Proc Natl Acad Sci USA 92*:8259–8263.

Betz SF, Bryson JW, DeGrado WF. 1995. Native-like and structurally characterized designed α-helical bundles. *Curr Opin Struct Biol 5*:457–463.

Blondelle SE, Ostresh JM, Houghton RA, Pérez-Payá E. 1995. Induced conformational states of amphipathic peptides in aqueous/lipid environments. *Biophys J 68*:351–359.

Chang CT, Wu C-SC, Yang JT. 1978. Circular dichroic analysis. *Anal Biochem 91*:13–31.

Chao H, Bautista DL, Litowski J, Irvin RT, Hodges RS. 1998. Use of a heterodimeric coiled-coil system for biosensor application and affinity purification. *J Chromatogr B 715*:307–329.

Chen Y-H, Yang JT, Chau KH. 1974. Determination of the helix and β form of proteins in aqueous solution by circular dichroism. *Biochemistry 13*:3350–3359.

Chong PCS, Hodges RS. 1982. Proximity of sulfhydryl groups to the sites of interaction between components of the troponin complex from rabbit skeletal muscle. *J Biol Chem 257*:2549–2555.

Cohen C, Parry DAD. 1990. α-Helical coiled coils and bundles: How to design an α-helical protein. *Proteins Struct Funct Genet 7*:1–15.

Cohn EJ, Edsall JT. 1943. *Proteins, amino acids and peptides as ions and dipolar ions.* New York: Reinhold.

Cooper TM, Woody RW. 1990. The effect of conformation on the CD of interacting helices: A theoretical study of tropomyosin. *Biopolymers 30*:657–676.

Crick FHC. 1953. The packing of α-helices: Simple coiled-coils. *Acta Crystallogr 6*:689–698.

Dill KA, Bromberg S, Yue K, Fiebig KM, Yee DP, Thomas PD, Chan HS. 1995. Principles of protein folding—A perspective from simple exact models. *Protein Sci 4*:561–602.

Eisenberg D, McLachlan AD. 1986. Solvation energy in protein folding and binding. *Nature 319*:199–203.

Eriksson AE, Baase WA, Zhang X-J, Heinz DW, Blaber M, Baldwin EP, Matthews BW. 1992. Response of a protein structure to cavity-creating mutations and its relation to the hydrophobic effect. *Science 255*:178–183.

Fauchère J-L, Pliska V. 1983. Hydrophobic parameters π of amino acid side chains from the partitioning of *N*-acetyl-amino-acid amides. *Eur J Med Chem 18*:369–375.

Glover L, Harrison S. 1995. Crystal structure of the heterodimeric BZIP transcription factor c-*fos*-c-*jun* bound to DNA. *Nature 373*:257–261.

Gonzalez L Jr, Brown RA, Richardson D, Alber T. 1996a. Crystal structures of a single coiled-coil peptide in two oligomeric states reveal the basis for structural polymorphism. *Nat Struct Biol 3*:1002–1009.

Gonzalez L Jr, Plecs JJ, Alber T. 1996b. An engineered allosteric switch in leucine-zipper oligomerization. *Nat Struct Biol 3*:510–515.

Gonzalez L Jr, Woolfson DN, Alber T. 1996c. Buried polar residues and structural specificity in the GCN4 leucine zipper. *Nat Struct Biol 3*:1011–1018.

Greenfield NJ, Hitchcock-DeGregori SE. 1995. The stability of tropomyosin, a two-stranded coiled-coil protein, is primarily a function of the hydrophobicity of residues at the helix-helix interface. *Biochemistry 34*:16797–16805.

Greenfield NJ, Montelione GT, Farid RS, Hitchcock-DeGregori SE. 1998. The structure of the N-terminus of striated muscle α-tropomyosin in a chimeric peptide: Nuclear magnetic resonance structure and circular dichroism studies. *Biochemistry 37*:7834–7843.

Guo D, Mant CT, Taneja AK, Parker R, Hodges RS. 1986. Prediction of peptide retention times in reversed-phase high-performance liquid chromatography I. Determination of retention coefficients of amino acid residues of model synthetic peptides. *J Chromatogr 359*:499–517.

Harbury PB, Zhang T, Kim PS, Alber T. 1993. A switch between two-, three-, and four-stranded coiled coils in GCN4 leucine zipper mutants. *Science 262*:1401–1407.

Hodges RS. 1992. Unzipping the secrets of coiled-coils. *Curr Biol 2*:122–124.

Hodges RS. 1996. De novo design of a-helical proteins: Basic research to medical applications. *Biochem Cell Biol 74*:133–154.

Hodges RS, Saund AK, Chong PCS, St.-Pierre SA, Reid RE. 1981. Synthetic model for two-stranded α-helical coiled-coils: Design, synthesis and characterization of an 86-residue analog of tropomyosin. *J Biol Chem 256*:1214–1224.

Hodges RS, Zhou NE, Kay CM, Semchuk PD. 1990. Synthetic model proteins: Contribution of hydrophobic residues and disulfide bonds to protein stability. *Pept Res 3*:123–137.

Johnson ML, Correia JJ, Yphantis DA, Halvorson HR. 1981. Analysis of data from the analytical ultracentrifuge by nonlinear least-squares techniques. *Biophys J 36*:575–588.

Junius FK, Mackay JP, Bubb WA, Jensen SA, Weiss AS, King GF. 1995. Nuclear magnetic resonance characterization of the Jun leucine zipper domain: Unusual properties of coiled-coil interfacial polar residues. *Biochemistry 34*:6164–6174.

Kammerer RA. 1997. α-Helical coiled-coil oligomerization domains in extracellular proteins. *Matrix Biol 15*:555–565.

Kammerer RA, Schulthess T, Landwehr R, Lustig A, Fischer D, Engel J. 1998. Tenascin-C hexabrachion assembly is a sequential two-step process initiated by coiled-coil α-helices. *J Biol Chem 273*:10602–10608.

Kohn WD, Hodges RS. 1998. *De novo* design of α-helical coiled-coils and bundles: Models for the development of protein-design principles. *Trends Biotechnol 16*:379–389.

Kohn WD, Kay CM, Hodges RS. 1995. Protein destabilization by electrostatic repulsions in the two-stranded α-helical coiled-coil/leucine zipper. *Protein Sci 4*:237–250.

Kohn WD, Kay CM, Hodges RS. 1998. Orientation, positional, additivity, and oligomerization-state effects of interhelical ion pairs in α-helical coiled-coils. *J Mol Biol 283*:993–1012.

Kohn WD, Mant CT, Hodges RS. 1997. α-Helical protein assembly motifs. *J Biol Chem 272*:2583–2586.

Lau SYM, Taneja AK, Hodges RS. 1984. Synthesis of a model protein of defined secondary and quaternary structure: Effect of chain length on the stabilization and formation of two-stranded α-helical coiled-coils. *J Biol Chem 259*:13253–13261.

Lavigne P, Crumo MP, Cagné SM, Hodges RS, Kay CM, Sykes BD. 1998. Insights into the mechanism of heterodimerization from the ^{1}H-NMR solution structure of the c-Myc-Max heterodimeric leucine zipper. *J Mol Biol 281*:165–181.

Lavigne P, Crump MP, Cagné SM, Sykes BD, Hodges RS, Kay CM. 1997. ^{1}H-NMR evidence for two buried Asn side-chains in the c-Myc-Max heterodimeric α-helical coiled-coil. *Technol Protein Chem 8*:617–624.

Lavigne P, Kondejewski LH, Michael E, Houston J, Sonnichsen FD, Lix B, Sykes BD, Hodges RS, Kay CM. 1995. Preferential heterodimeric parallel coiled-coil formation by synthetic Max and c-Myc leucine zippers: A description of putative electrostatic interactions responsible for the specificity of heterodimerization. *J Mol Biol 254*:505–520.

Lee KH, Xie D, Freire E, Amzel LM. 1994. Estimation of changes in side-chain configurational entropy in binding and folding: General methods and application to helix formation. *Proteins Struct Funct Genet 20*:68–84.

Lovejoy B, Choe S, Cascio D, McRorie DK, DeGrado WF, Eisenberg D. 1993. Crystal structure of a synthetic triple-stranded α-helical bundle. *Science 259*:1288–1293.

Lumb KJ, Kim PS. 1995. A buried polar interaction imparts structural uniqueness in a designed heterodimeric coiled coil. *Biochemistry 34*:8642–8648.

Lupas A. 1996. Coiled coils: New structures and new functions. *Trends Biochem Res 21*:375–382.

Lupas A. 1997. Predicting coiled-coil regions in proteins. *Curr Opin Struct Biol 7*:388–393.

Lupas A, Van Dyke M, Stock J. 1991. Predicting coiled coils from protein sequences. *Science 252*:1162–1164.

Matthews BW. 1993. Structural and genetic analysis of protein stability. *Annu Rev Biochem 62*:139–160.

Moitra J, Szilák L, Krylov D, Vinson C. 1997. Leucine is the most stabilizing aliphatic amino acid in the d position of a dimeric leucine zipper coiled coil. *Biochemistry 36*:12567–12573.

Monera OD, Kay CM, Hodges RS. 1994a. Electrostatic interactions control the parallel and antiparallel orientation of α-helical chains in two-stranded α-helical coiled-coils. *Biochemistry 33*:38692–3871.

Monera OD, Kay CM, Hodges RS. 1994b. Protein denaturation with guanidine hydrochloride or urea provides a different estimate of stability depending on the contribution of electrostatics. *Protein Sci 3*:1984–1991.

Monera OD, Sereda TJ, Zhou NE, Kay CM, Hodges RS. 1995. Relationship of sidechain hydrophobicity and α-helical propensity on the stability of the single-stranded amphipathic α-helix. *J Peptide Sci 1*:319–329.

Monera OD, Sönnichsen FD, Hicks L, Kay CM, Hodges RS. 1996. The relative positions of alanine residues in the hydrophobic core control the formation of two-stranded or four-stranded α-helical coiled-coils. *Protein Eng 9*:353–363.

Monera OD, Zhou NE, Kay CM, Hodges RS. 1993. Comparison of antiparallel and parallel two-stranded α-helical coiled-coils: Design, synthesis and characterization. *J Biol Chem 268*:19218–19227.

Morjana NA, McKeone BJ, Gilbert HF. 1993. Guanidine hydrochloride stabilization of a partially unfolded intermediate during the reversible denaturation of protein disulfide isomerase. *Proc Natl Acad Sci USA 90*:2107–2111.

Muhle-Goll C, Gibson T, Schuck P, Schubert D, Nalis D, Nilges M, Pastore A. 1994. The dimerization stability of the HLH-LZ transcription protein family is modulated by the leucine zipper: A CD and NMR study of TFEB and c-Myc. *Biochemistry 33*:11296–11306.

Muñoz V, Serrano L. 1996. Local versus nonlocal interactions in protein folding and stability—An experimentalist's point of view. *Folding Design 1*:R71–R77.

Myers JK, Pace CN, Scholtz JM. 1995. Denaturant *m* values and heat capacity changes: Relation to changes in accessible surface areas of protein unfolding. *Protein Sci 4*:2138–2148.

Nicholls A, Sharp KA, Honig B. 1991. Protein folding and association: Insights from the interfacial and thermodynamic properties of hydrocarbons. *Proteins Struct Funct Genet 11*:281–296.

O'Shea EK, Klemm JD, Kim PS, Alber T. 1991. X-ray structure of the GCN4 leucine zipper, a two-stranded, parallel coiled coil. *Science 254*:539–544.

O'Shea EK, Rutkowski R, Kim PS. 1989. Evidence that the leucine zipper is a coiled coil. *Science 243*:538–542.

Pace CN. 1986. Determination and analysis of urea and guanidinium hydrochloride denaturation curves. *Methods Enzymol 131*:266–280.

Richards FM, Lim WA. 1994. An analysis of packing in the protein folding problem. *Q Rev Biophys 26*:423–498.

Sali D, Baycroft M, Fersht AR. 1991. Surface electrostatic interactions contribute little to stability of barnase. *J Mol Biol 220*:779–788.

Sönnichsen FD, Van Eyk JE, Hodges RS, Sykes BD. 1992. Effect of trifluoroethanol on protein secondary structure: An NMR and CD study using a synthetic actin peptide. *Biochemistry 31*:8790–8798.

Su JY, Hodges RS, Kay CM. 1994. Effect of chain length on the formation and stability of synthetic α-helical coiled-coils. *Biochemistry 33*:15501–15510.

Thompson KS, Vinson CR, Freire E. 1993. Thermodynamic characterization of the structural stability of the coiled-coil region of the bZIP transcription factor GCN4. *Biochemistry 32*:5491–5496.

Tripet B, Vale RD, Hodges RS. 1997. Demonstration of coiled-coil interactions within the kinesin neck region using synthetic peptides: Implications for motor activity. *J Biol Chem 272*:8946–8956.

Wagschal K, Tripet B, Hodges RS. 1999. *De novo* design of a model peptide sequence to examine the effects of single amino acid substitutions in the hydrophobic core on both stability and oligomerization state of coiled-coils. *J Mol Biol 285*:785–803.

Weissenhorn W, Dessen A, Harrison SC, Skehel JJ, Wiley DC. 1997. Atomic structure of the ectodomain from HIV-1 gp41. *Nature 387*:426–430.

Wishart DS, Boyco RF, Willard L, Richards FM, Sykes B. 1994. SEQSEE: A comprehensive program suite for protein sequence analysis. *Comp Appl Biosci 10*:121–132.

Wolf E, Kim PS, Berger B. 1997. MultiCoil: A program for predicting two- and three-stranded coiled coils. *Protein Sci 6*:1179–1189.

Woolfson DN, Alber T. 1995. Predicting oligomerization states of coiled coils. *Protein Sci 4*:1596–1607.

Yphantis DA. 1991. *Nonlinear least squares program for analysis of equilibrium ultracentrifugation experiments*. David A. Yphantis, 99 River Rd., Mansfield Center, Connecticut 06250-1018.

Zeng X, Zhu H, Lashuel HA, Hu JC. 1997. Oligomerization properties of GCN4 leucine zipper **e** and **g** position mutants. *Protein Sci 6*:2218–2226.

Zhou NE, Kay CM, Hodges RS. 1992a. Synthetic model proteins: Positional effects of interchain hydrophobic interactions on stability of two-stranded α-helical coiled coils. *J Biol Chem 267*:2664–2670.

Zhou NE, Kay CM, Hodges RS. 1992b. Synthetic model proteins: The relative contribution of leucine residues at the nonequivalent positions of the 3–4 hydrophobic repeat to the stability of the two-stranded α-helical coiled-coil. *Biochemistry 31*:5739–5746.

Zhou NE, Mant CT, Hodges RS. 1990. Effect of preferred binding domains on peptide retention behavior in reversed-phase chromatography: Amphipathic α-helices. *Peptide Res 3*:8–20.

Zhou NE, Monera OD, Kay CM, Hodges RS. 1994. α-Helical propensities of amino acids in the hydrophobic face of an amphipathic α-helix. *Protein Pept Lett 1*:114–119.

Zhu B-Y, Zhou NE, Kay CM, Hodges RS. 1993. Packing and hydrophobicity effects on protein folding and stability: Effects of β-branched amino acids, valine and isoleucine, on the formation and stability of two-stranded a-helical coiled-coils/leucine zippers. *Protein Sci 2*:383–394.